

CHAPTER-4

RESULTS AND DISCUSSION

4.1 Introduction

The effect of network components on Signal to Crosstalk plus Noise ratio (SCNR) considering combined effect of crosstalk and noise in the long-haul optical communication system is analyzed and analytical expressions are presented for evaluating Bit Error Rate (BER) and Power Penalty (PP) performance in the previous chapters. Following the analytical formulations, in this chapter, the effect of various parameters such as received power, number of wavelengths per fiber and number of fibers on system performance is presented. To get the induced BER performance of a WDM network using L-WIXC architectures and optical pre-amplifier in each hop, equation (3.31) is utilized through the equations (3.11)~(3.30). The BER performance trend is analyzed for determining the PP performance trend for the same system parameters. Finally, from the PP performance trend, the effect on maximum number of allowable hops for specific system parameters is determined.

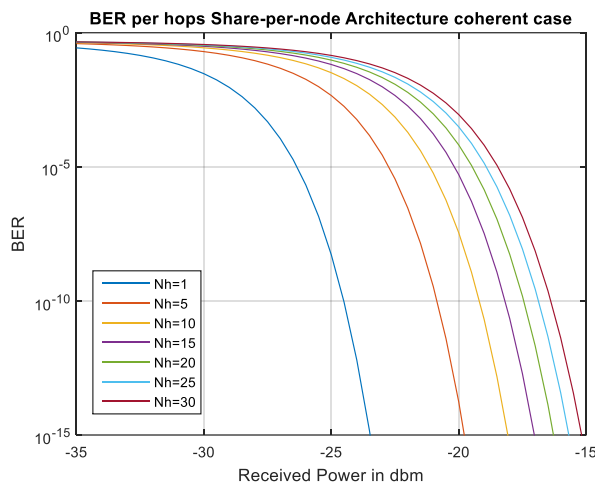
4.2 BER Performance Trend

The effect of received power on BER performance pattern varying the number of hops has been achieved for the following cases respectively in Fig. 4.1.

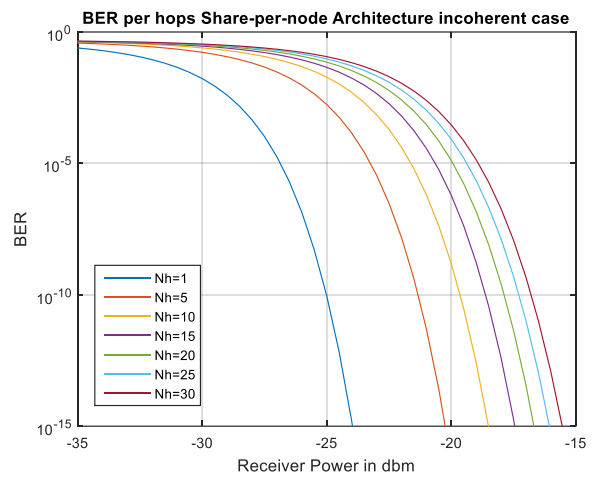
- a. Share per node coherent case
- b. Share per node incoherent case
- c. Share per link coherent case
- d. Share per link incoherent case
- e. DCS-1 coherent case

- f. DCS-1 incoherent case
- g. DCS-2 coherent case
- h. DCS-2 incoherent case
- i. Wavelength switch OXC coherent case
- j. Wavelength switch OXC incoherent case
- k. MWSF coherent case
- l. MWSF incoherent case

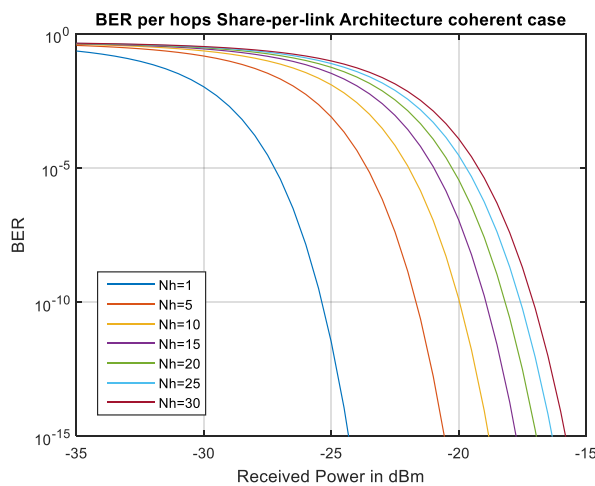
The variation of BER with received power graphs presented below are assumed for **80 Km hop length**, 32 input fibers and 16 wavelengths.



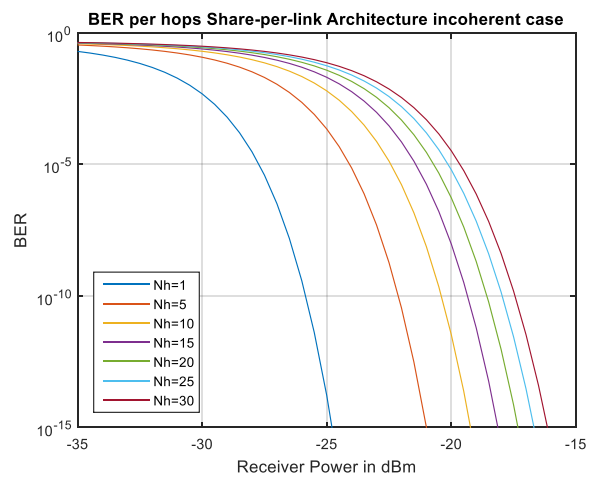
(a)



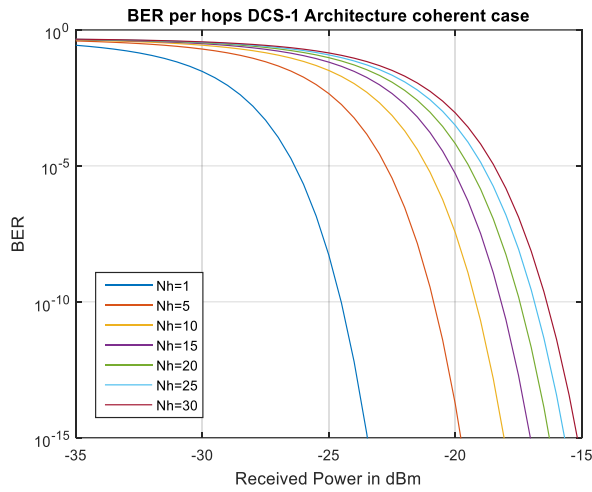
(b)



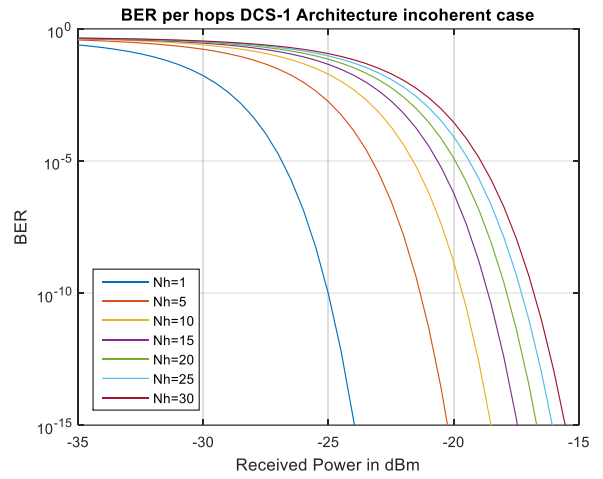
(c)



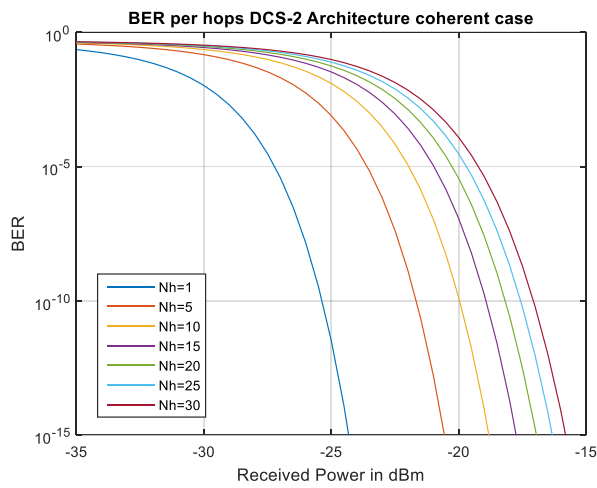
(d)



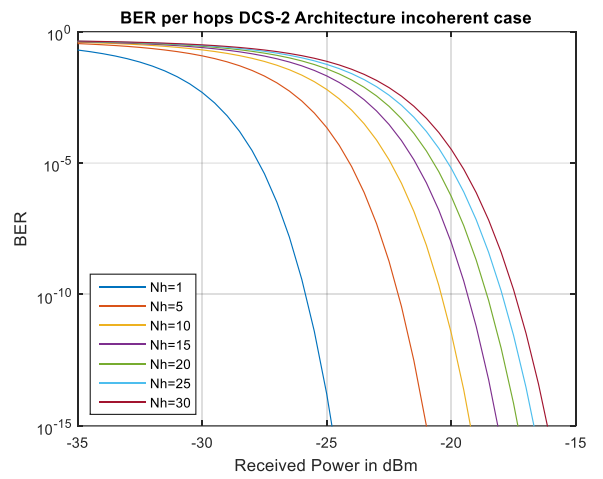
(e)



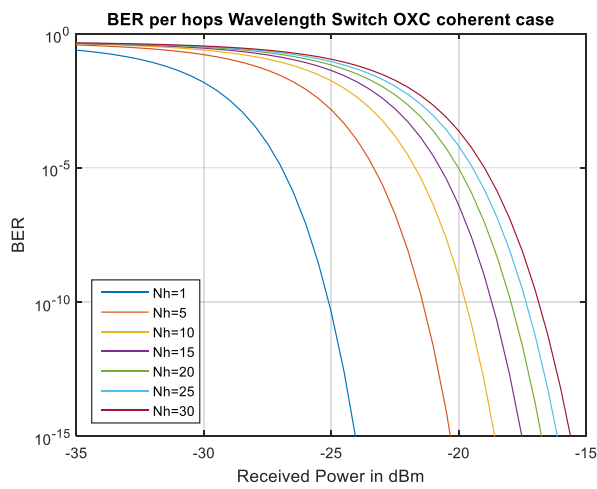
(f)



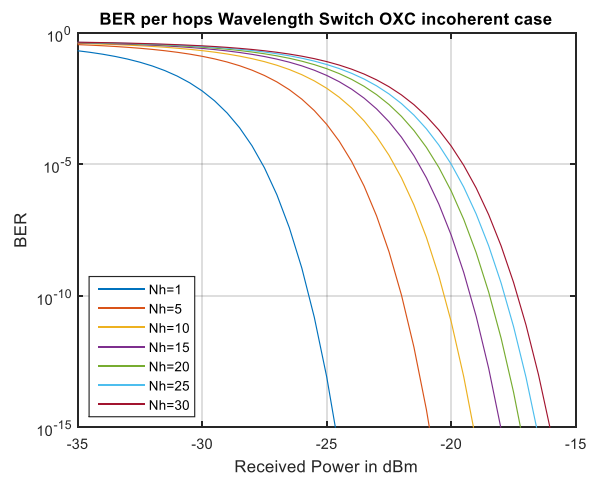
(g)



(h)



(i)



(j)

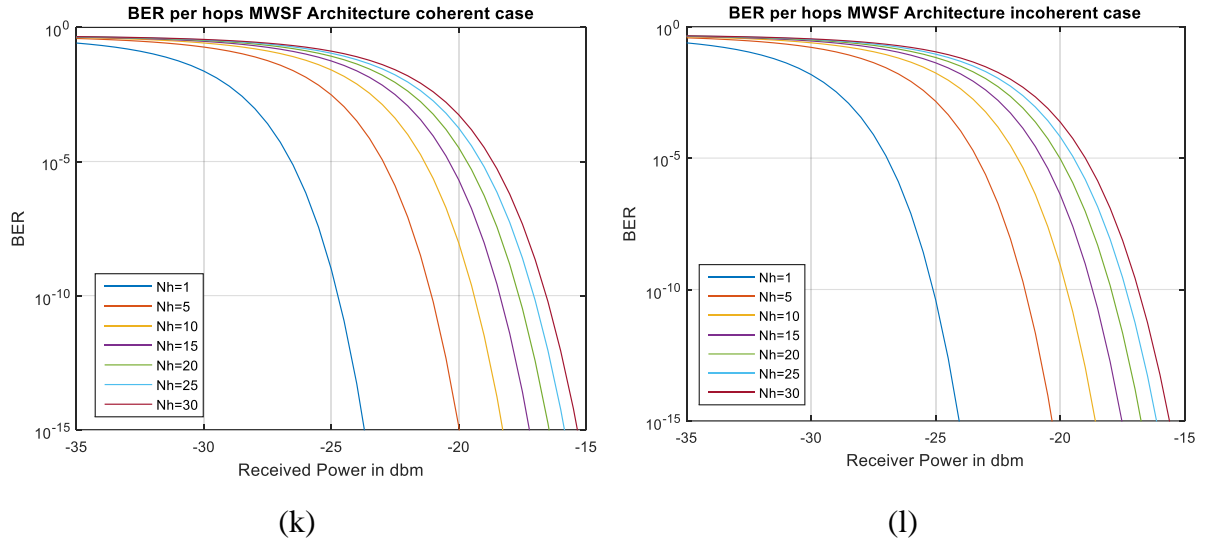


Fig. 4.1 Variation of BER with Received power for varying number of hops using Different L-WIXC architectures ($N=32$, $M=16$, $C_n=4$, $\delta=-20\text{dBm}$, $\varepsilon=-25\text{dBm}$, $\varepsilon'=-25\text{dBm}$)

Fig 4.1 (a)-(l) shows the variation of BER with received power for different number of hops for a particular number of wavelengths and number of input fibers. We have achieved the BER performance pattern depending on the received power varying the number of hops in a WDM system using six different L-WIXC architectures for both coherent and incoherent cases respectively. In above figures, number of input fiber is $N=32$, number of wavelengths per fiber $M=16$ and number of converters per link $C_n=4$; optical powers relative to the actual signal of the crosstalk contribution from the tunable filter/ Multiwavelength selective filter (MWSF), switch both first and second stage (in case of wavelength switch OXC) and second stage switch (in case of share-per-node architecture and DCS-1) are -20 dBm , -25 dBm and -25 dBm respectively. It is observed that, to achieve the same BER, increase of received power is required with the increase of number of hops since the amplifier induced noise and crosstalk accumulates through the number of hops travelled by the signal. It is also found that the same BER is achievable in same L-WIXC architecture with less receiver sensitivity in incoherent case than in coherent case for a particular number of hops.

4.3 Evaluation of Power Penalty

In this previous section, the BER performance trend is presented for a particular number of wavelengths per fiber, M and number of input fiber, N. Following the above, the BER performance trend while varying values of M and N depending on various number of hops is analyzed here. From the BER performance curves, the variation of received powers at specific BER of 10^{-9} is determined depending on the combination of values of N and M. For the power penalty analysis, equation (3.29) is modified by putting $\sigma_{T0} = \sqrt{\sigma_{Th}^2 + \sigma_{Sh}^2}$ (Without Crosstalk and Amplifier Noise) and used in equations (3.30) and (3.31) to find out the Received Power Without Crosstalk value at $BER_0 = 10^{-9}$. The numerical values of received power varying number of hops, number of wavelength channels and number of input fibers are then used to find out PP for different L-WIXC architectures which are presented in the subsequent sections.

4.4 Power Penalty Trend for Share per Node L-WIXC Architecture

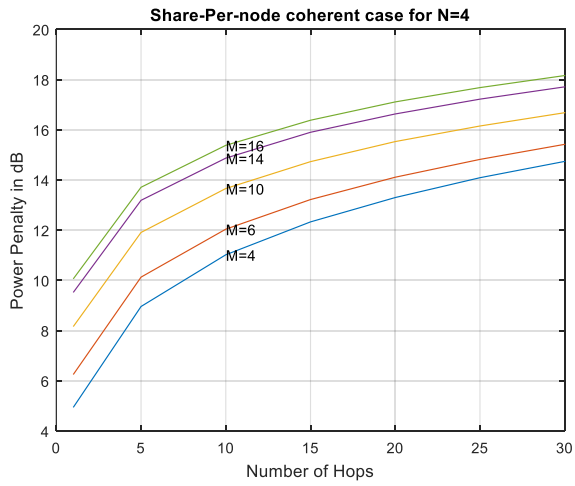
The BER versus Received Power graph in Fig. 4.1(a) and 4.1(b) is analyzed varying number of wavelengths in a fiber using M=4, 6, 10, 14, 16 keeping number of fiber, N fixed to find out the received power variation at BER of 10^{-9} for various number of hops for both coherent and incoherent cases of Share-per Node L-WIXC architectures. Then the same analysis is carried out for different values number of input fibers using N=4, 8, 16, 24 and 32 for all the above-mentioned number of wavelengths. The values of received power at BER of 10^{-9} are shown in Table I.

TABLE I

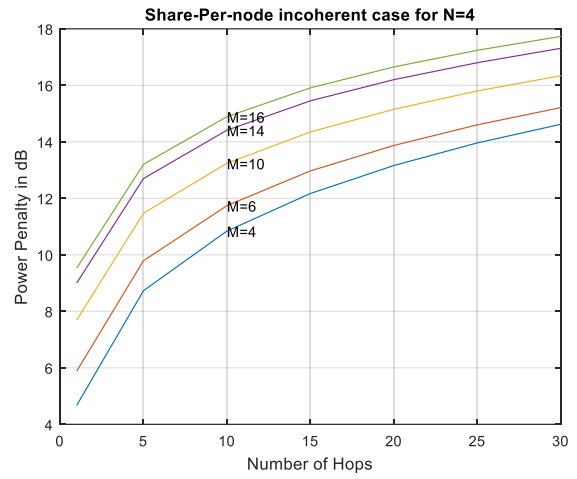
BER PERFORMANCE TREND FOR SHARE PER NODE L-WIXC ARCHITECTURE

Number of Hops	N=4; M=4	N=4; M=10	N=4; M=16	N=16; M=4	N=16; M=10	N=16; M=16	N=32; M=4	N=32; M=10	N=32; M=16
Share per Node Coherent Case									
1	-30.02	-26.8	-24.9	-29.37	-26.64	-24.84	-29	-26.54	-24.8
5	-26	-23.05	-21.25	-25.42	-22.91	-21.19	-25.1	-22.82	-21.14
10	-23.94	-21.3	-19.58	-23.44	-21.17	-19.52	-23.16	-21.08	-19.48
15	-22.63	-20.23	-18.58	-22.2	-20.1	-18.52	-21.94	-20.01	-18.48
20	-21.66	-19.43	-17.85	-21.27	-19.32	-17.8	-21.04	-19.24	-17.76
25	-20.87	-18.81	-17.28	-20.52	-18.7	-17.22	-20.32	-18.61	-17.19
30	-20.22	-18.28	-16.8	-19.9	-18.17	-16.75	-19.71	-18.1	-16.71
Share per Node Incoherent Case									
1	-30.29	-27.27	-25.43	-29.54	-27.08	-25.35	-29.16	-26.95	-25.3
5	-26.23	-23.49	-21.76	-25.58	-23.32	-21.68	-25.24	-23.2	-21.63
10	-24.12	-21.72	-20.07	-23.58	-21.55	-19.99	-23.28	-21.44	-19.95
15	-22.79	-20.61	-19.05	-22.33	-20.46	-18.98	-22.05	-20.36	-18.93
20	-21.8	-19.81	-18.31	-21.38	-19.66	-18.24	-21.14	-19.56	-18.2
25	-21	-19.16	-17.72	-20.63	-19.01	-17.65	-20.41	-18.93	-17.61
30	-20.34	-18.62	-17.23	-19.99	-18.48	-17.17	-19.8	-18.4	-17.12

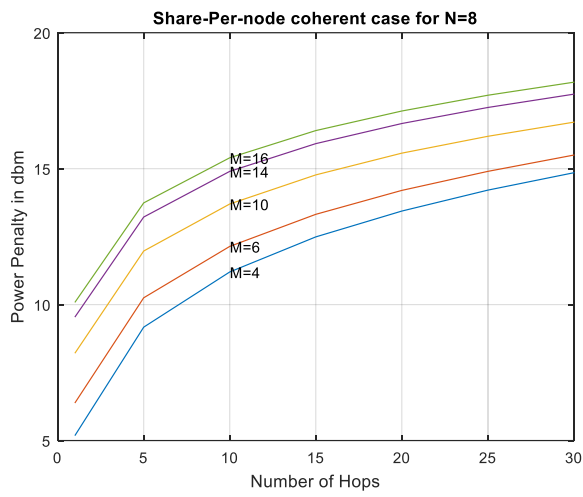
Now the received power values from Table I are analyzed to find out PP for various number of hops while wavelengths and input fibers are varied. The performance trend for a WDM network using Share per Node L-WIXC architecture as a function of number of hops varying number of input wavelengths, M for (a) Coherent Case when N=4 (b) Incoherent Case when N=4 (c) Coherent Case when N=8 (d) Incoherent Case when N=8 (e) Coherent Case when N=16 (f) Incoherent Case when N=16 (g) Coherent Case when N=24 (h) Incoherent Case when N=24 (i) Coherent Case when N=32 (j) Incoherent Case when N=32 is presented in Fig 4.2 below.



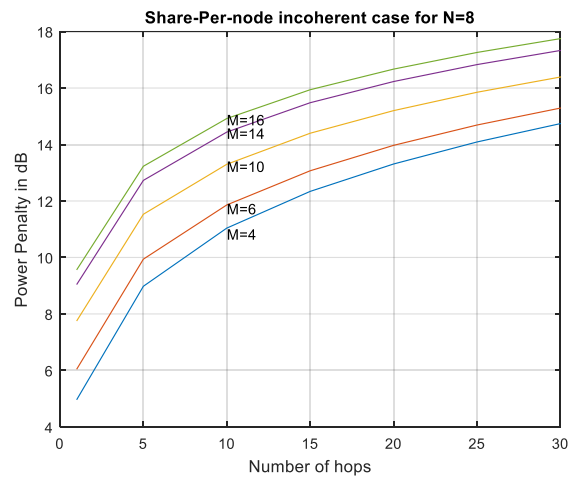
(a)



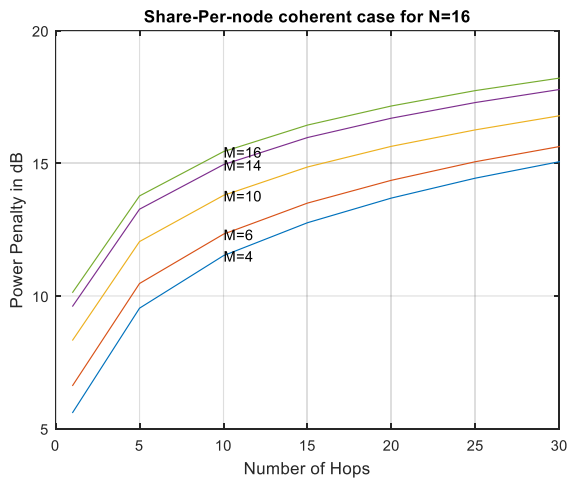
(b)



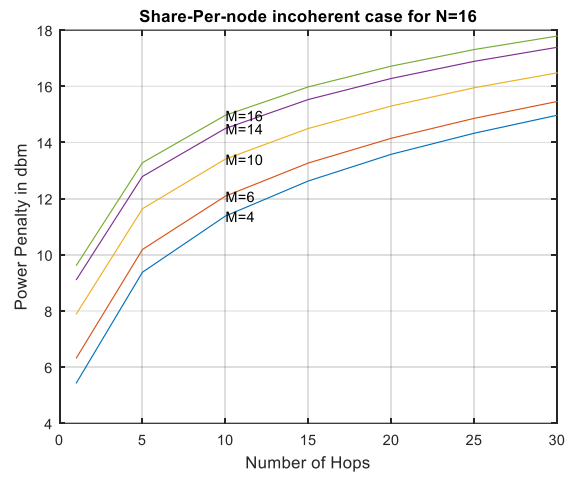
(c)



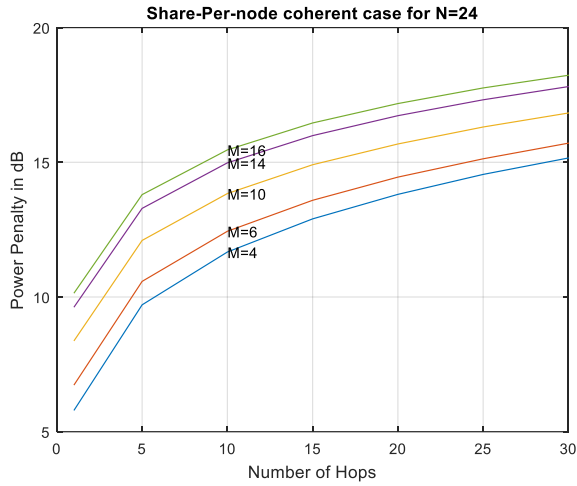
(d)



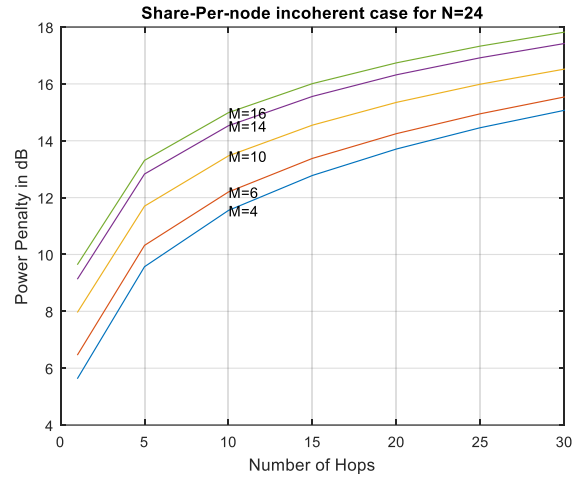
(e)



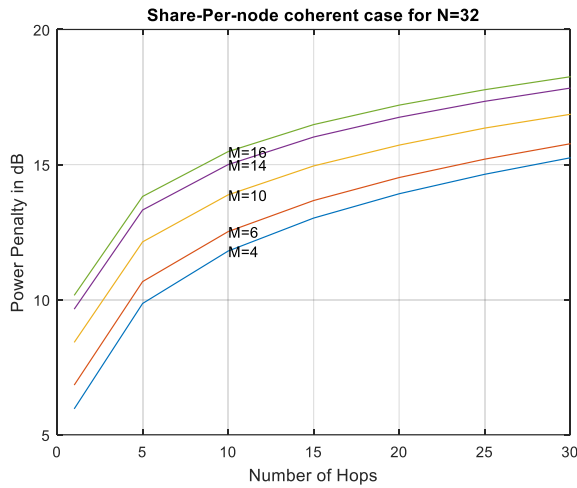
(f)



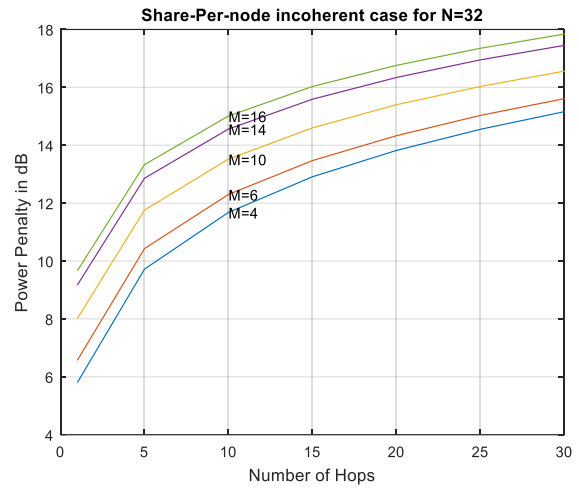
(g)



(h)



(i)



(j)

Fig. 4.2 Power penalty for a WDM network using **Share per Node** L-WIXC architecture as a function of number of hops varying number of input wavelengths for (a) Coherent Case when $N=4$ (b) Incoherent Case when $N=4$ (c) Coherent Case when $N=8$ (d) Incoherent Case when $N=8$ (e) Coherent Case when $N=16$ (f) Incoherent Case when $N=16$ (g) Coherent Case when $N=24$ (h) Incoherent Case when $N=24$ (i) Coherent Case when $N=32$ (j) Incoherent Case when $N=32$

From Fig 4.2, it is observed that when the signal passes through more hops, additional power penalty occurs since the receiver sensitivity decreases due to induced crosstalk and noise through the system for maintaining the same BER level. It is also observed that between these two cases of coherent and incoherent crosstalk, the more power penalty is found in coherent case than incoherent case with same number of hops and the same

number of wavelength channels. As the number of wavelength channel increases, the same amount of receiver power penalty is to be achieved by decreasing the number hops used in the system.

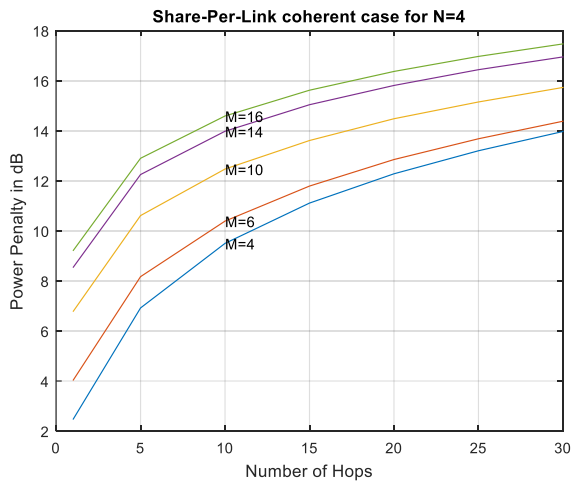
4.5 Power Penalty Trend for Share-per-Link L-WIXC Architecture

The BER versus Received Power graph in Fig. 4.1(c) and 4.1(d) is analyzed varying number of wavelengths in a fiber using $M=4, 6, 10, 14, 16$ keeping number of fiber, N fixed to find out the received power variation at BER of 10^{-9} for various number of hops for both coherent and incoherent cases of Share-per Link L-WIXC architectures. Then the same analysis is carried out for different values number of input fibers using $N=4, 8, 16, 24$ and 32 for all the above-mentioned number of wavelengths. The values of received power at BER of 10^{-9} are shown in Table II.

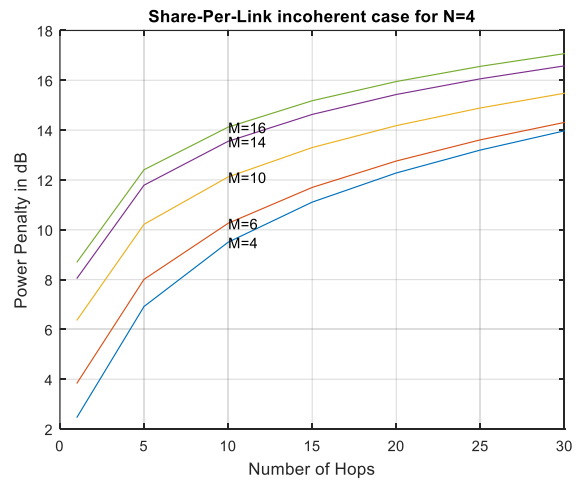
TABLE II
BER PERFORMANCE TREND FOR SHARE PER LINK L-WIXC ARCHITECTURE

Number of Hops	N=4; M=4	N=4; M=10	N=4; M=16	N=16; M=4	N=16; M=10	N=16; M=16	N=32; M=4	N=32; M=10	N=32; M=16
Share per Link Coherent Case									
1	-32.5	-28.19	-25.76	-31.41	-28.04	-25.71	-30.55	-27.86	-25.65
5	-28.04	-24.35	-22.06	-27.18	-24.22	-22.02	-26.46	-24.04	-21.96
10	-25.46	-22.49	-20.37	-24.87	-22.38	-20.33	-24.31	-22.22	-20.28
15	-23.85	-21.35	-19.34	-23.4	-21.23	-19.3	-22.94	-21.09	-19.25
20	-22.68	-20.48	-18.59	-22.32	-20.38	-18.54	-21.93	-20.25	-18.49
25	-21.76	-19.81	-17.99	-21.45	-19.71	-17.95	-21.12	-19.58	-17.9
30	-20.99	-19.23	-17.49	-20.74	-19.14	-17.45	-20.44	-19.02	-17.4
Share per Link Incoherent Case									
1	-32.5	-28.6	-26.27	-31.41	-28.42	-26.21	-30.55	-28.21	-26.13
5	-28.04	-24.74	-22.55	-27.18	-24.56	-22.49	-26.46	-24.37	-22.42
10	-25.46	-22.84	-20.84	-24.87	-22.7	-20.79	-24.31	-22.51	-20.72
15	-23.85	-21.66	-19.78	-23.4	-21.52	-19.74	-22.94	-21.36	-19.67
20	-22.68	-20.78	-19.01	-22.32	-20.65	-18.96	-21.93	-20.49	-18.9
25	-21.76	-20.07	-18.4	-21.45	-19.96	-18.36	-21.12	-19.82	-18.3
30	-20.99	-19.48	-17.89	-20.74	-19.38	-17.85	-20.44	-19.24	-17.79

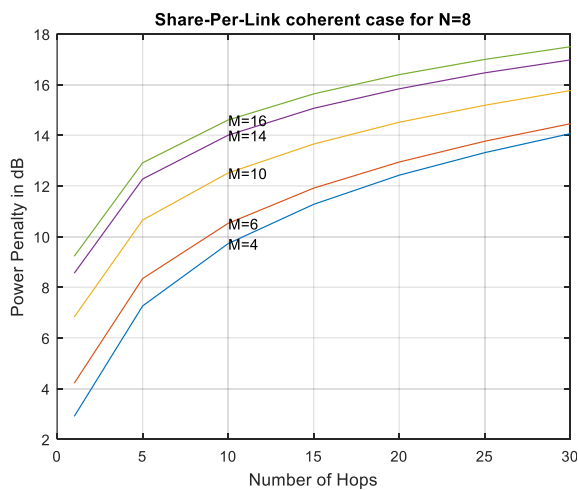
Power penalty performance trend for a WDM network using Share-per Link L-WIXC architecture as a function of number of hops varying number of input wavelengths, M for (a) Coherent Case when $N=4$ (b) Incoherent Case when $N=4$ (c) Coherent Case when $N=8$ (d) Incoherent Case when $N=8$ (e) Coherent Case when $N=16$ (f) Incoherent Case when $N=16$ (g) Coherent Case when $N=24$ (h) Incoherent Case when $N=24$ (i) Coherent Case when $N=32$ (j) Incoherent Case when $N=32$ has been presented in Fig 4.3 below.



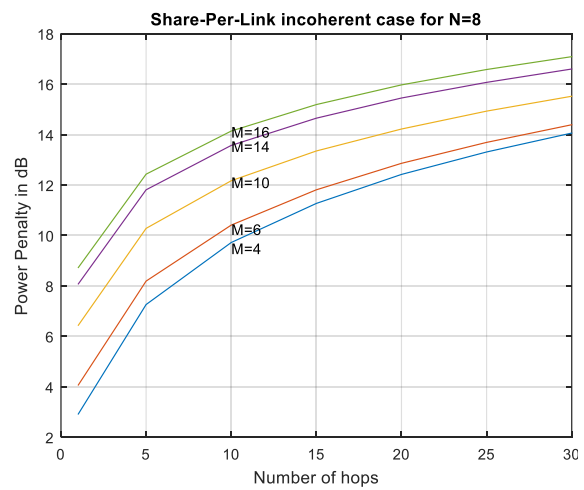
(a)



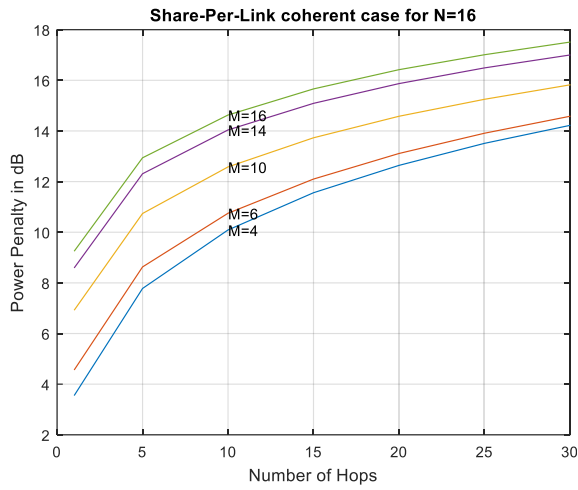
(b)



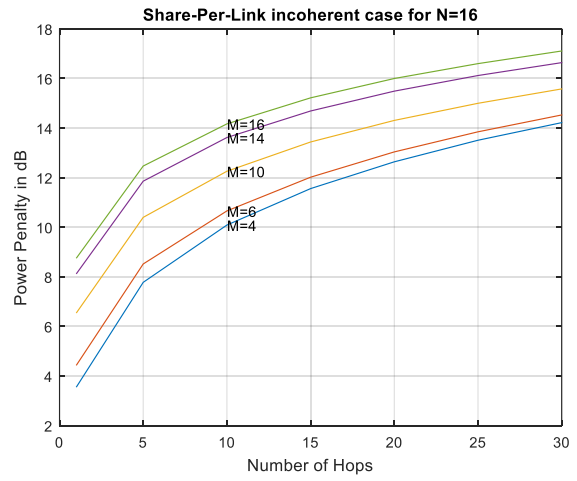
(c)



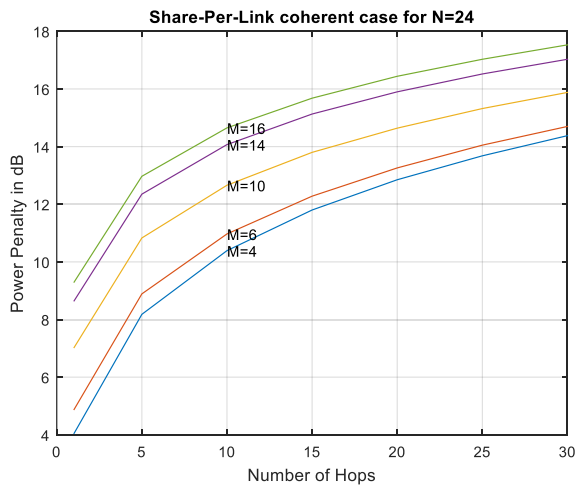
(d)



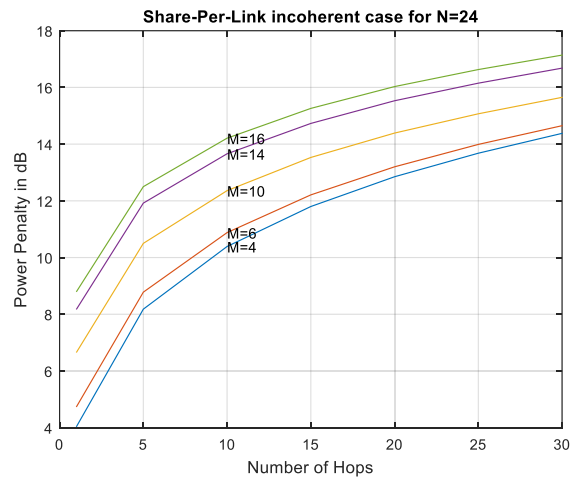
(e)



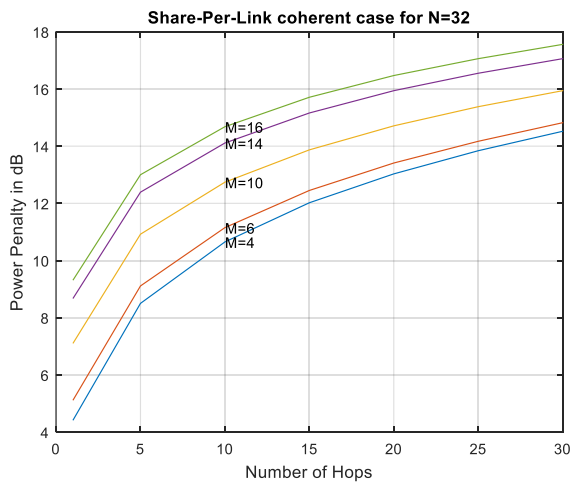
(f)



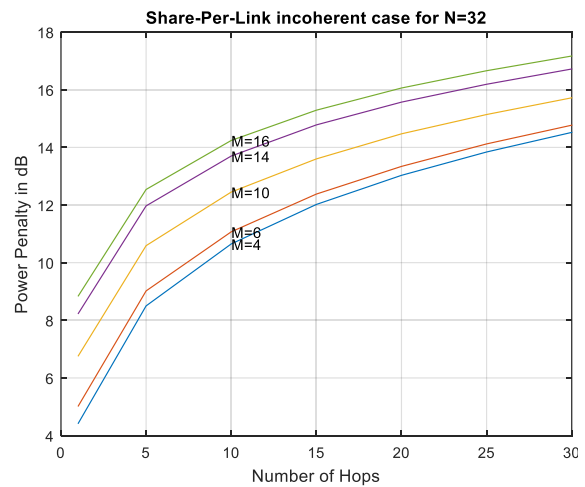
(g)



(h)



(i)



(j)

Fig. 4.3 Power penalty for a WDM network using **Share-per-Link** L-WIXC architecture as a function of number of hops varying number of input wavelengths for (a) Coherent Case when N=4 (b) Incoherent Case when N=4 (c) Coherent Case when N=8 (d)

Incoherent Case when N=8 (e) Coherent Case when N=16 (f) Incoherent Case when N=16 (g) Coherent Case when N=24 (h) Incoherent Case when N=24 (i) Coherent Case when N=32 (j) Incoherent Case when N=32.

From Fig 4.3, it is observed that when the signal passes through more hops, additional power penalty occurs since the receiver sensitivity decreases due to induced crosstalk and noise through the system for maintaining the same BER level. It is also observed that between these two cases of coherent and incoherent crosstalk, the more power penalty is found in coherent case than incoherent case with same number of hops and the same number of wavelength channels. As the number of wavelength channel increases, the same amount of receiver power penalty is to be achieved by decreasing the number hops used in the system.

4.6 Power Penalty Trend for DCS-1 L-WIXC Architecture

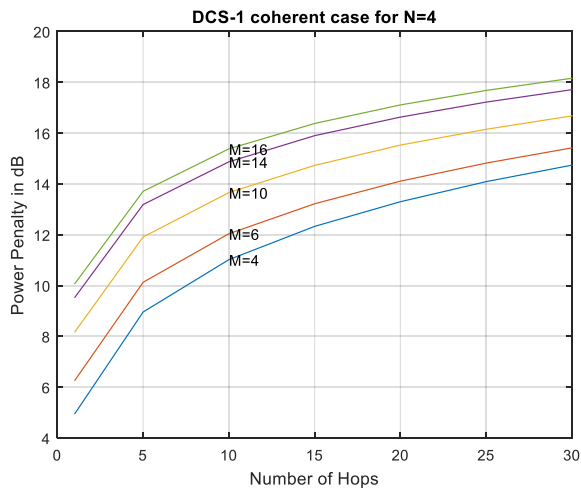
The BER versus Received Power graph in Fig. 4.1(e) and 4.1(f) is analyzed varying number of wavelengths in a fiber using M=4, 6, 10, 14, 16 keeping number of fiber, N fixed to find out the received power variation at BER of 10^{-9} for various number of hops for both coherent and incoherent cases of DCS-1 L-WIXC architectures. Then the same analysis is carried out for different values number of input fibers using N=4, 8, 16, 24 and 32 for all the above-mentioned number of wavelengths. The values of received power at BER of 10^{-9} are shown in Table III.

TABLE III
BER PERFORMANCE TREND FOR DCS-1 L-WIXC ARCHITECTURE

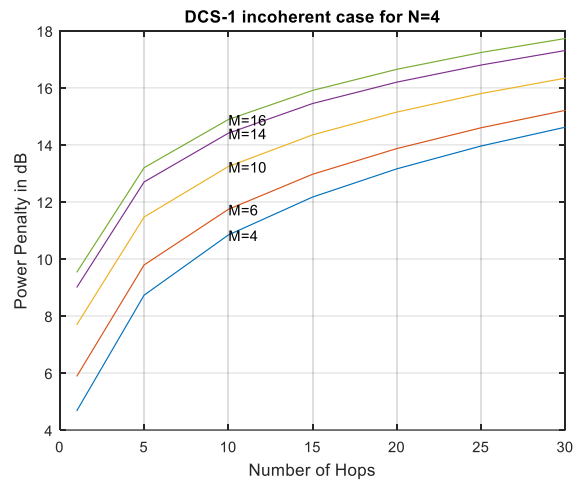
Number of Hops	N=4; M=4	N=4; M=10	N=4; M=16	N=16; M=4	N=16; M=10	N=16; M=16	N=32; M=4	N=32; M=10	N=32; M=16
DCS-1 Coherent Case									
1	-30.02	-26.8	-24.9	-29.37	-26.64	-24.84	-29	-26.54	-24.8
5	-26	-23.05	-21.25	-25.42	-22.91	-21.19	-25.1	-22.82	-21.14
10	-23.94	-21.3	-19.58	-23.44	-21.17	-19.52	-23.16	-21.08	-19.48
15	-22.63	-20.23	-18.58	-22.2	-20.1	-18.52	-21.94	-20.01	-18.48

20	-21.66	-19.43	-17.85	-21.27	-19.32	-17.8	-21.04	-19.24	-17.76
25	-20.87	-18.81	-17.28	-20.52	-18.7	-17.22	-20.32	-18.61	-17.19
30	-20.22	-18.28	-16.8	-19.9	-18.17	-16.75	-19.71	-18.1	-16.71
DCS-1 Incoherent Case									
1	-30.29	-27.27	-25.43	-29.54	-27.08	-25.35	-29.16	-26.95	-25.3
5	-26.23	-23.49	-21.76	-25.58	-23.32	-21.68	-25.24	-23.2	-21.63
10	-24.12	-21.72	-20.07	-23.58	-21.55	-19.99	-23.28	-21.44	-19.95
15	-22.79	-20.61	-19.05	-22.33	-20.46	-18.98	-22.05	-20.36	-18.93
20	-21.8	-19.81	-18.31	-21.38	-19.66	-18.24	-21.14	-19.56	-18.2
25	-21	-19.16	-17.72	-20.63	-19.01	-17.65	-20.41	-18.93	-17.61
30	-20.34	-18.62	-17.23	-19.99	-18.48	-17.17	-19.8	-18.4	-17.12

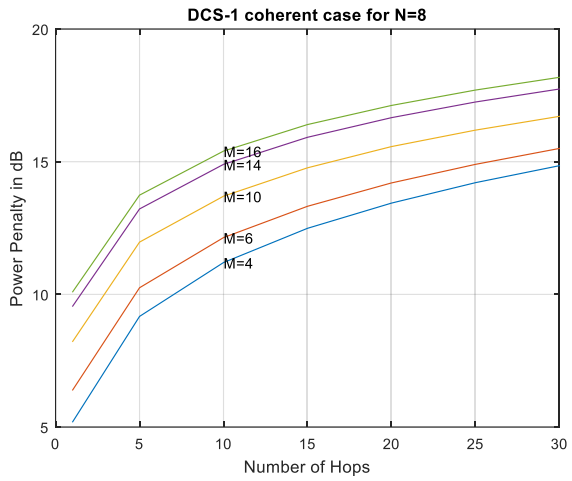
Power penalty performance trend for a WDM network using DCS-1 L-WIXC architecture as a function of number of hops varying number of input wavelengths, M for (a) Coherent Case when N=4 (b) Incoherent Case when N=4 (c) Coherent Case when N=8 (d) Incoherent Case when N=8 (e) Coherent Case when N=16 (f) Incoherent Case when N=16 (g) Coherent Case when N=24 (h) Incoherent Case when N=24 (i) Coherent Case when N=32 (j) Incoherent Case when N=32 is presented in Fig 4.4 below.



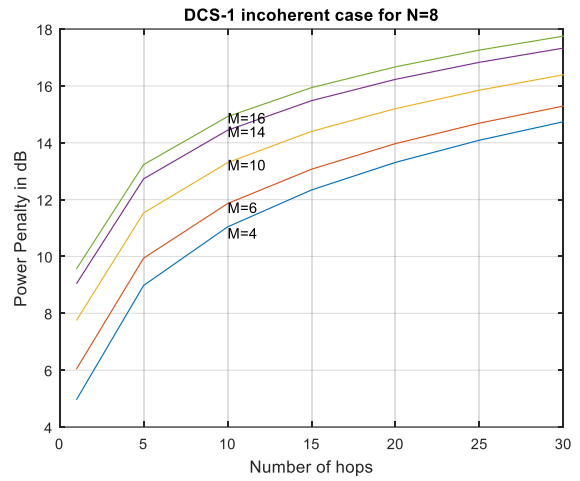
(a)



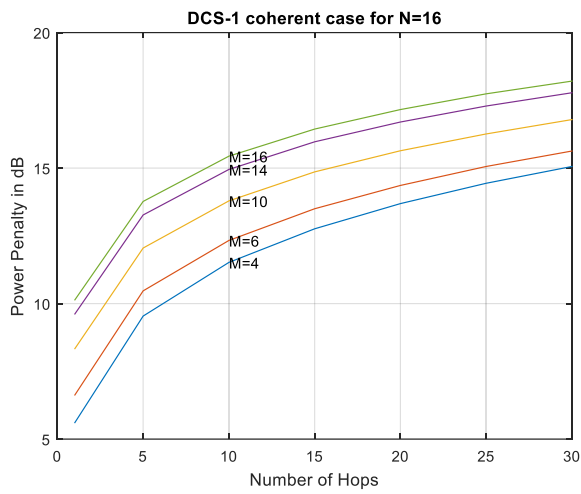
(b)



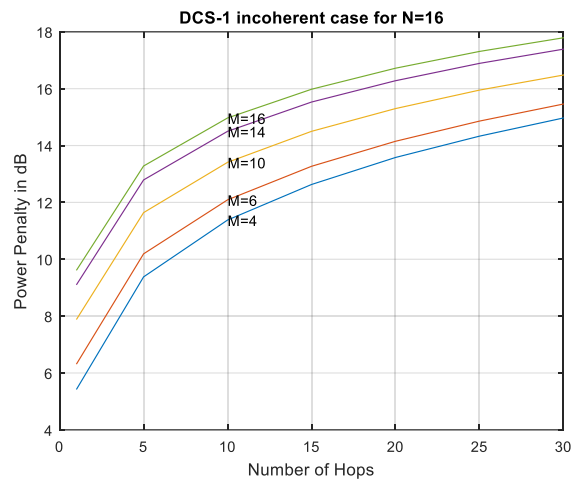
(c)



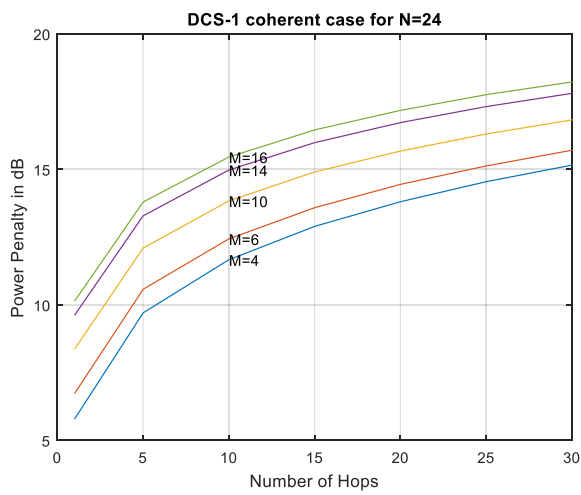
(d)



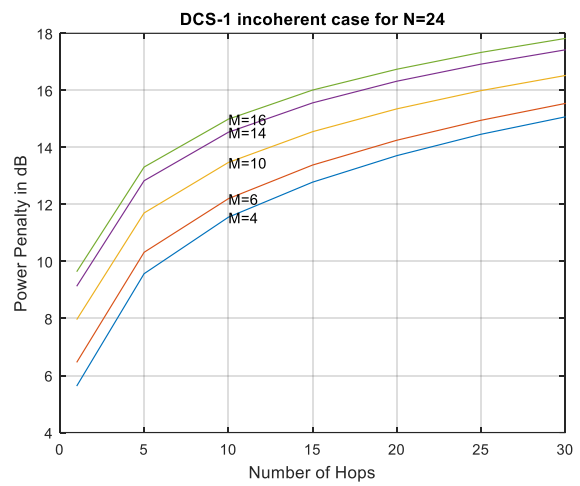
(e)



(f)



(g)



(h)

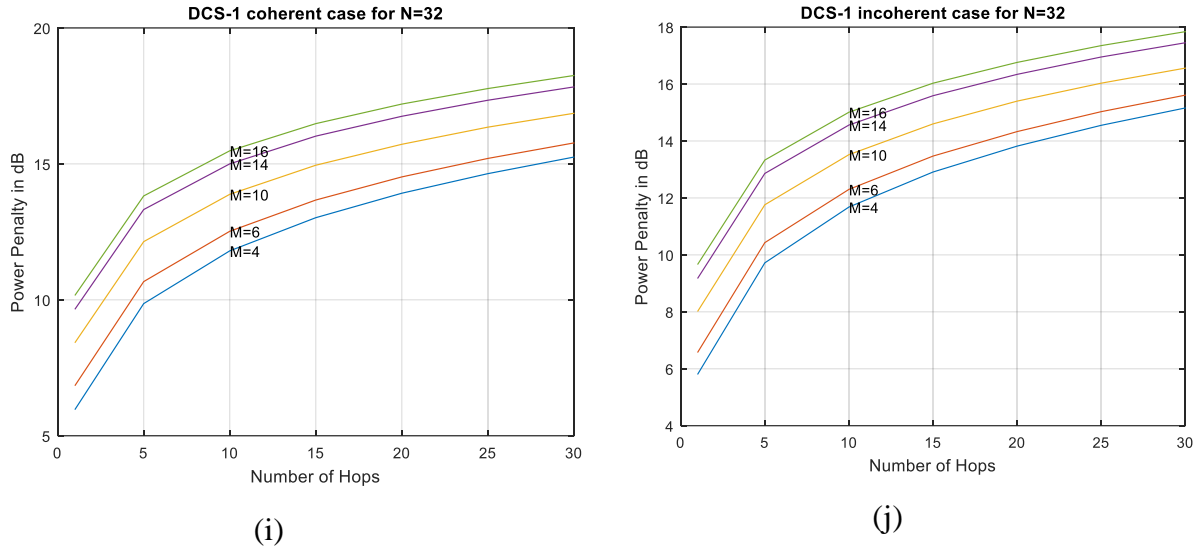


Fig. 4.4 Power penalty for a WDM network using **DCS-1** L-WIXC architecture as a function of number of hops varying number of input wavelengths for (a) Coherent Case when N=4 (b) Incoherent Case when N=4 (c) Coherent Case when N=8 (d) Incoherent Case when N=8 (e) Coherent Case when N=16 (f) Incoherent Case when N=16 (g) Coherent Case when N=24 (h) Incoherent Case when N=24 (i) Coherent Case when N=32 (j) Incoherent Case when N=32

From Fig 4.4 it is observed that, when the signal passes through more hops, additional power penalty occurs since the receiver sensitivity decreases due to induced crosstalk and noise through the system for maintaining the same BER level. It is also observed that between these two cases of coherent and incoherent crosstalk, the more power penalty is found in coherent case than incoherent case with same number of hops and the same number of wavelength channels. As the number of wavelength channel increases, the same amount of receiver power penalty is to be achieved by decreasing the number hops used in the system.

4.7 Power Penalty Trend for DCS-2 L-WIXC Architecture

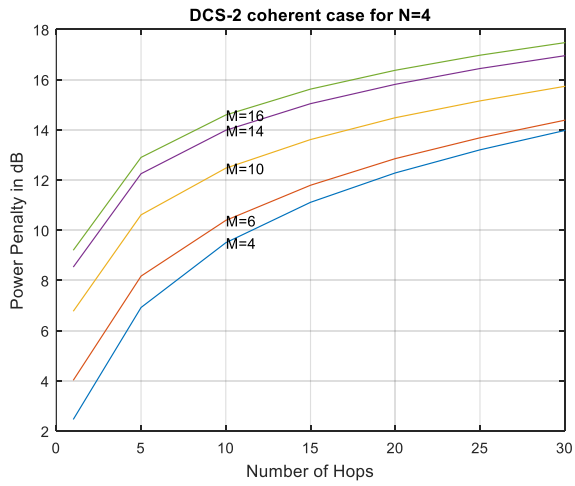
The BER versus Received Power graphs in Fig. 4.1(g) and 4.1(h) are analyzed varying number of wavelengths in a fiber using M=4, 6, 10, 14, 16 keeping number of fiber, N fixed to find out the received power variation at BER of 10^{-9} for various number of hops for both

coherent and incoherent cases of DCS-2 L-WIXC architectures. Then the same analysis is carried out for different values number of input fibers using N=4, 8, 16, 24 and 32 for all the above-mentioned number of wavelengths. The values of received power at BER of 10^{-9} are shown in Table IV.

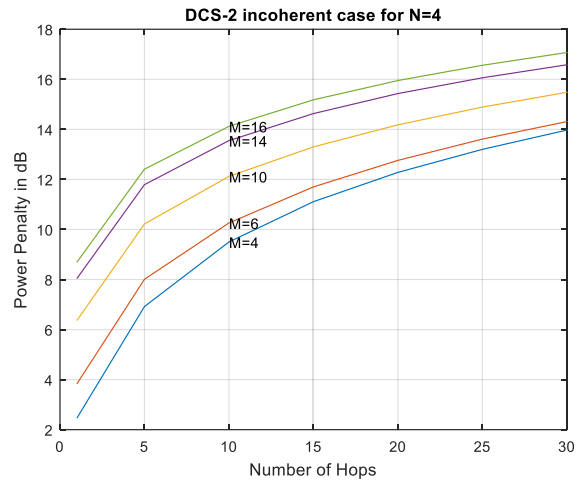
TABLE IV
BER PERFORMANCE TREND FOR DCS-2 L-WIXC ARCHITECTURE

Number of Hops	N=4; M=4	N=4; M=10	N=4; M=16	N=16; M=4	N=16; M=10	N=16; M=16	N=32; M=4	N=32; M=10	N=32; M=16
DCS-2 Coherent Case									
1	-32.5	-28.19	-25.76	-31.41	-28.04	-25.71	-30.55	-27.86	-25.65
5	-28.04	-24.35	-22.06	-27.18	-24.22	-22.02	-26.46	-24.04	-21.96
10	-25.46	-22.49	-20.37	-24.87	-22.38	-20.33	-24.31	-22.22	-20.28
15	-23.85	-21.35	-19.34	-23.4	-21.23	-19.3	-22.94	-21.09	-19.25
20	-22.68	-20.48	-18.59	-22.32	-20.38	-18.54	-21.93	-20.25	-18.49
25	-21.76	-19.81	-17.99	-21.45	-19.71	-17.95	-21.12	-19.58	-17.9
30	-20.99	-19.23	-17.49	-20.74	-19.14	-17.45	-20.44	-19.02	-17.4
DCS-2 Incoherent Case									
1	-32.5	-28.6	-26.27	-31.41	-28.42	-26.21	-30.55	-28.21	-26.13
5	-28.04	-24.74	-22.55	-27.18	-24.56	-22.49	-26.46	-24.37	-22.42
10	-25.46	-22.84	-20.84	-24.87	-22.7	-20.79	-24.31	-22.51	-20.72
15	-23.85	-21.66	-19.78	-23.4	-21.52	-19.74	-22.94	-21.36	-19.67
20	-22.68	-20.78	-19.01	-22.32	-20.65	-18.96	-21.93	-20.49	-18.9
25	-21.76	-20.07	-18.4	-21.45	-19.96	-18.36	-21.12	-19.82	-18.3
30	-20.99	-19.48	-17.89	-20.74	-19.38	-17.85	-20.44	-19.24	-17.79

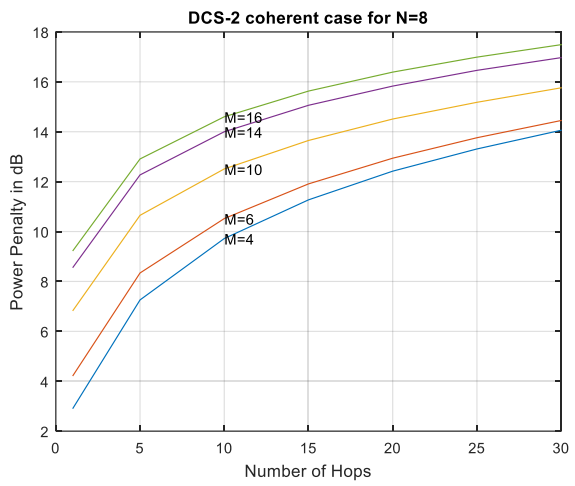
Power penalty performance trend for a WDM network using DCS-2 L-WIXC architecture as a function of number of hops varying number of input wavelengths, M for (a) Coherent Case when N=4 (b) Incoherent Case when N=4 (c) Coherent Case when N=8 (d) Incoherent Case when N=8 (e) Coherent Case when N=16 (f) Incoherent Case when N=16 (g) Coherent Case when N=24 (h) Incoherent Case when N=24 (i) Coherent Case when N=32 (j) Incoherent Case when N=32 is presented in Fig 4.5 below.



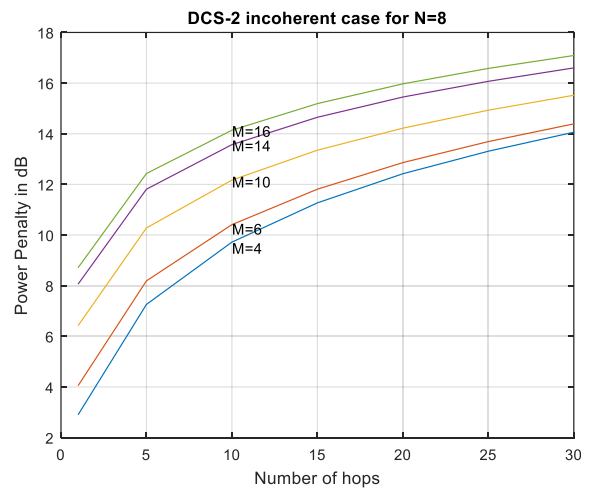
(a)



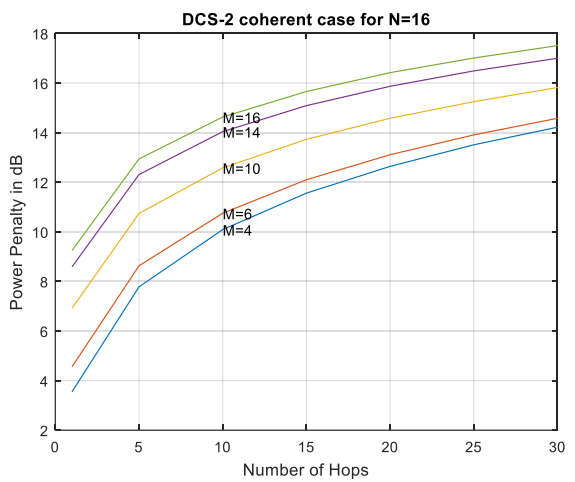
(b)



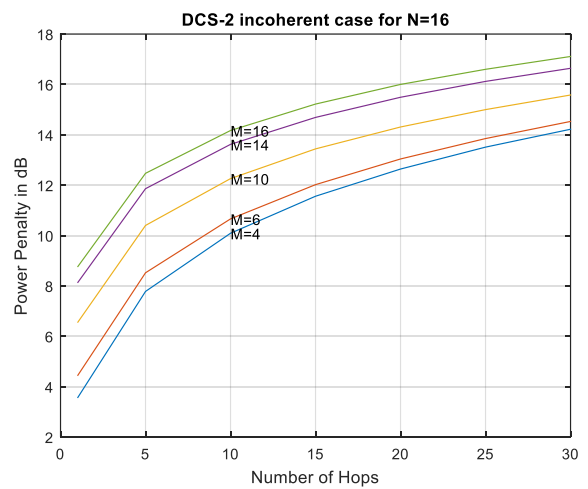
(c)



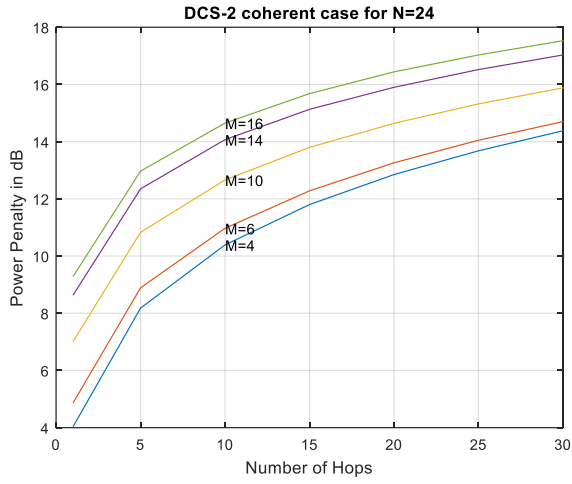
(d)



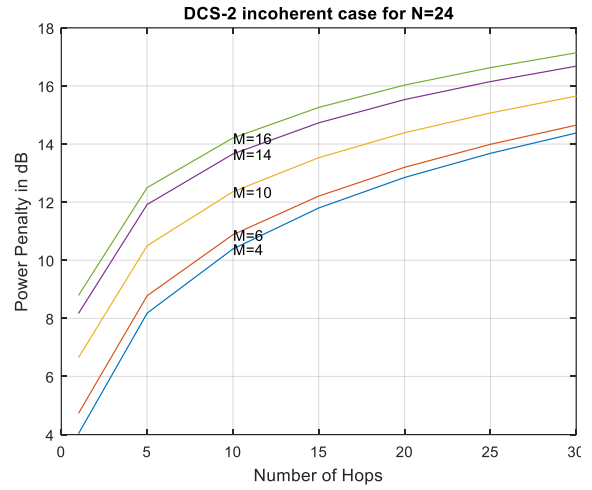
(e)



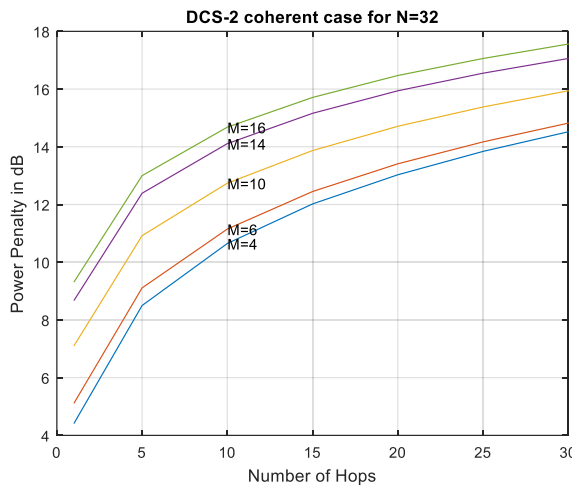
(f)



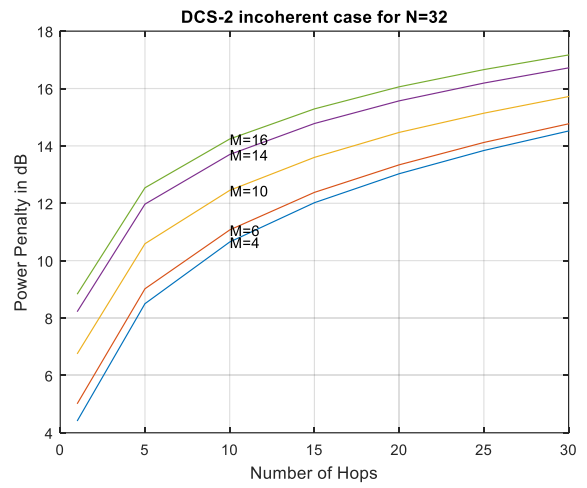
(g)



(h)



(i)



(j)

Fig. 4.5 Power penalty for a WDM network using **DCS-2** L-WIXC architecture as a function of number of hops varying number of input wavelengths for (a) Coherent Case when $N=4$ (b) Incoherent Case when $N=4$ (c) Coherent Case when $N=8$ (d) Incoherent Case when $N=8$ (e) Coherent Case when $N=16$ (f) Incoherent Case when $N=16$ (g) Coherent Case when $N=24$ (h) Incoherent Case when $N=24$ (i) Coherent Case when $N=32$ (j) Incoherent Case when $N=32$.

From Fig. 4.5 it is observed that, when the signal passes through more hops, additional power penalty occurs since the receiver sensitivity decreases due to induced crosstalk and noise through the system for maintaining the same BER level. It is also observed that between these two cases of coherent and incoherent crosstalk, the more power penalty is found in coherent case than incoherent case with same number of hops and the same

number of wavelength channels. As the number of wavelength channel increases, the same amount of receiver power penalty is to be achieved by decreasing the number hops used in the system.

4.8 Power Penalty Trend for WS-based L-WIXC Architecture

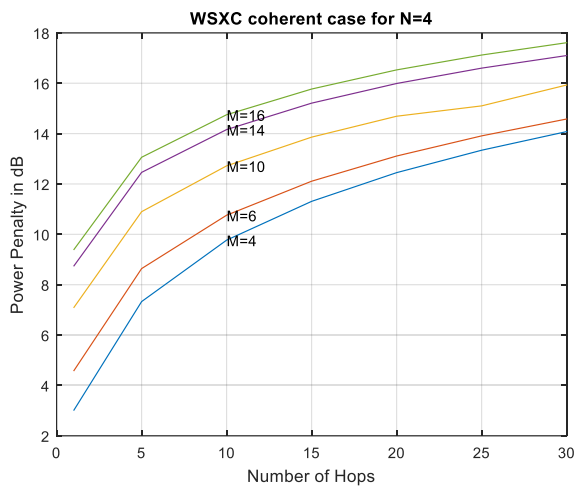
The BER versus Received Power graphs in Fig. 4.1(i) and 4.1(j) are analyzed varying number of wavelengths in a fiber using $M=4, 6, 10, 14, 16$ keeping number of fiber, N fixed to find out the received power variation at BER of 10^{-9} for various number of hops for both coherent and incoherent cases of WSXC architectures. Then the same analysis is carried out for different values number of input fibers using $N=4, 8, 16, 24$ and 32 for all the above-mentioned number of wavelengths. The values of received power at BER of 10^{-9} are shown in Table V.

TABLE V

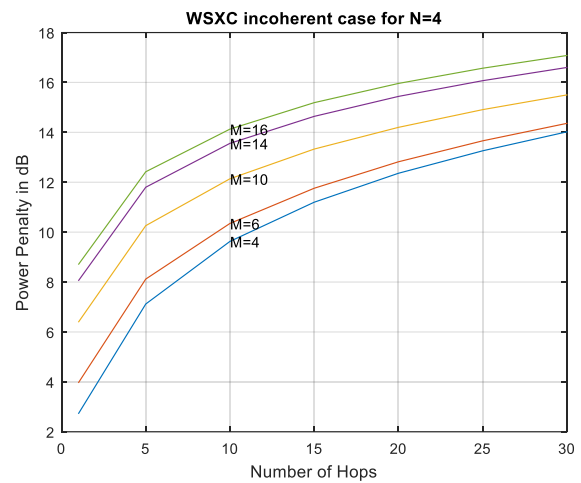
BER PERFORMANCE TREND FOR WAVELENGTH SWITCH-BASED L-WIXC ARCHITECTURE

Number of Hops	N=4; M=4	N=4; M=10	N=4; M=16	N=16; M=4	N=16; M=10	N=16; M=16	N=32; M=4	N=32; M=10	N=32; M=16
Wavelength Switch-based Coherent Case									
1	-31.96	-27.88	-25.58	-30.5	-27.63	-25.49	-29.49	-27.34	-25.39
5	-27.63	-24.06	-21.9	-26.42	-23.83	-21.82	-25.53	-23.56	-21.71
10	-25.19	-22.24	-20.21	-24.28	-22.02	-20.13	-23.54	-21.78	-20.03
15	-23.65	-21.1	-19.19	-22.92	-20.91	-19.11	-22.28	-20.68	-19.01
20	-22.51	-20.27	-18.43	-21.91	-20.08	-18.36	-21.35	-19.86	-18.27
25	-21.62	-19.859	-17.84	-21.1	-19.42	-17.78	-20.6	-19.21	-17.69
30	-20.88	-19.03	-17.35	-20.42	-18.87	-17.28	-19.96	-18.67	-17.19
Wavelength Switch-based Incoherent Case									
1	-32.24	-28.57	-26.26	-25.49	-28.23	-26.14	-29.56	-27.85	-25.99
5	-27.84	-24.7	-22.54	-21.82	-24.39	-22.43	-25.59	-24.03	-22.30
10	-25.33	-22.82	-20.83	-20.13	-22.53	-20.72	-23.59	-22.21	-20.59
15	-23.76	-21.63	-19.77	-19.11	-21.37	-19.67	-22.33	-21.08	-19.54
20	-22.6	-20.76	-19.0	-18.36	-20.51	-18.91	-21.39	-20.24	-18.79
25	-21.7	-20.05	-18.39	-17.78	-19.83	-18.30	-20.64	-19.57	-18.18
30	-20.94	-19.46	-17.88	-17.28	-19.26	-17.79	-20.00	-19.00	-17.68

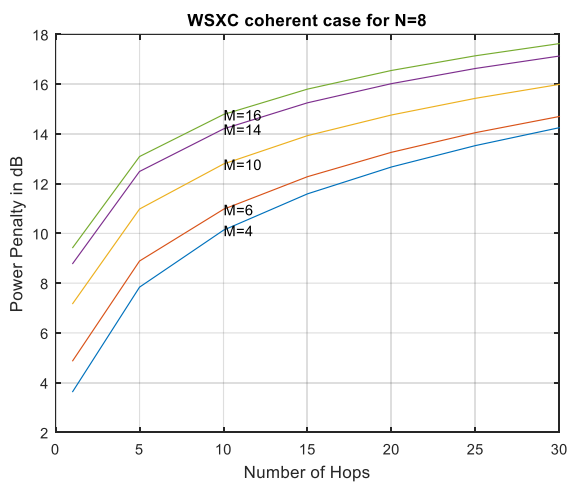
Power penalty performance trend for a WDM network using WS-based L-WIXC architecture as a function of number of hops varying number of input wavelengths, M for (a) Coherent Case when N=4 (b) Incoherent Case when N=4 (c) Coherent Case when N=8 (d) Incoherent Case when N=8 (e) Coherent Case when N=16 (f) Incoherent Case when N=16 (g) Coherent Case when N=24 (h) Incoherent Case when N=24 (i) Coherent Case when N=32 (j) Incoherent Case when N=32 has been presented in Fig 4.6 below.



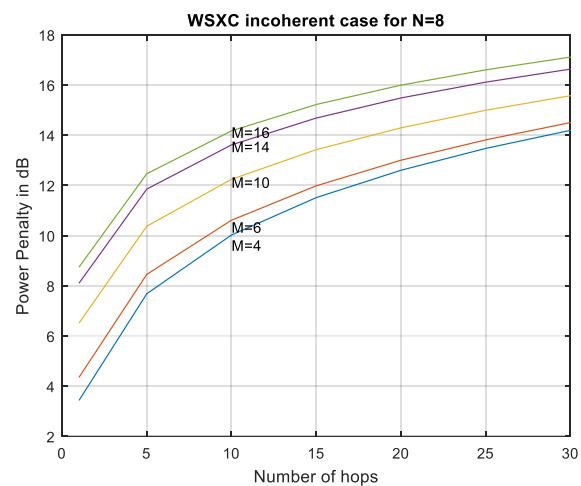
(a)



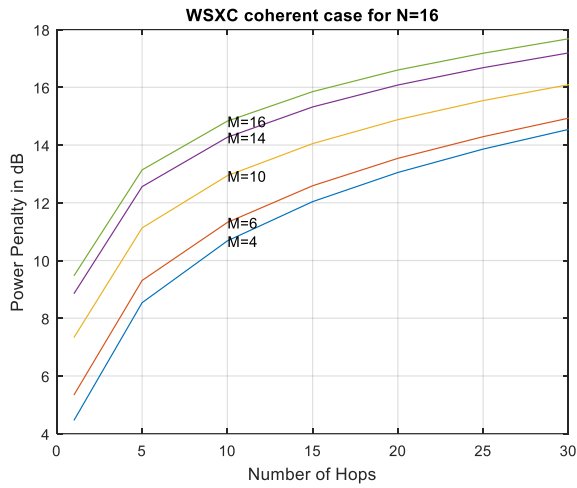
(b)



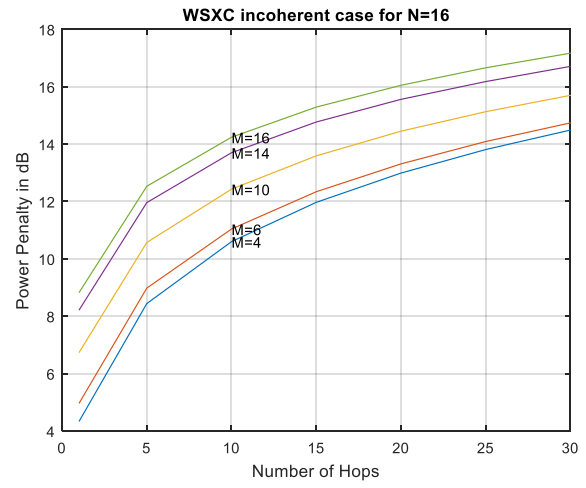
(c)



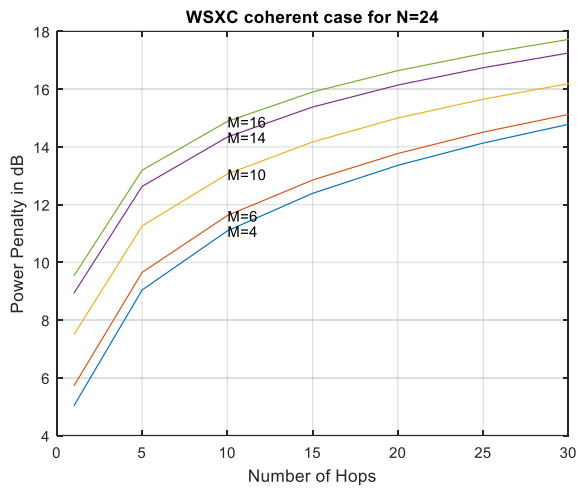
(d)



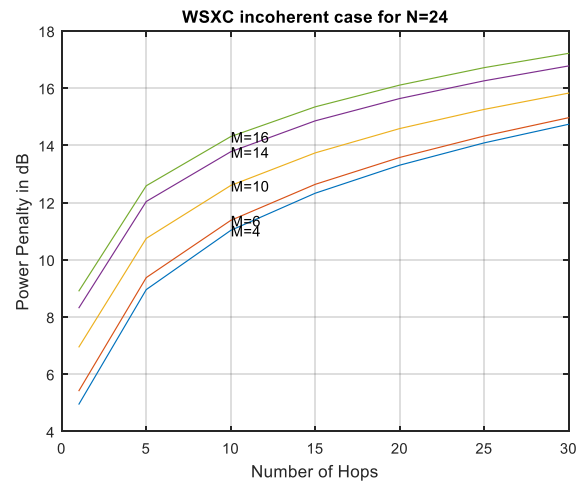
(e)



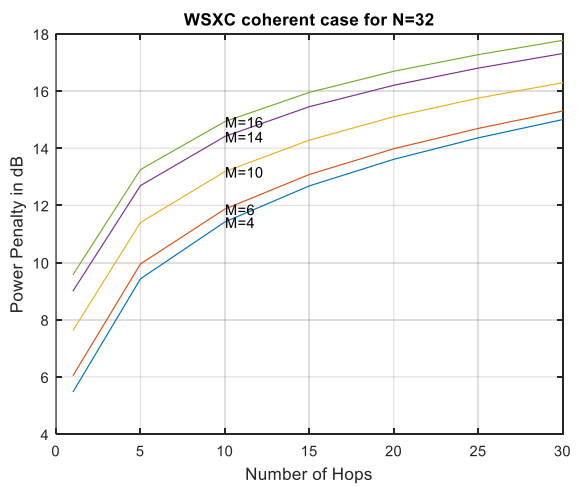
(f)



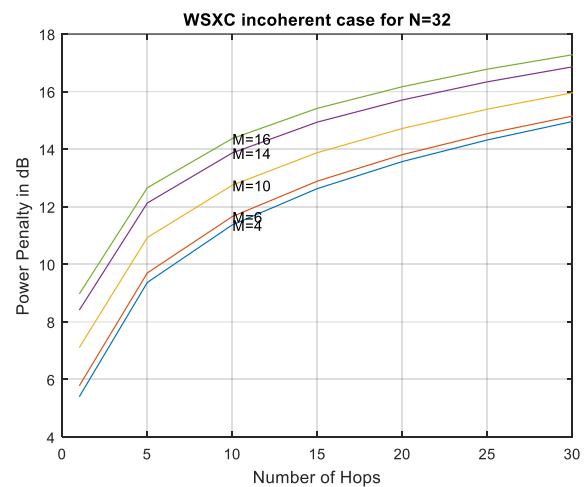
(g)



(h)



(i)



(j)

Fig. 4.6 Power penalty for a WDM network using Wavelength Switching-based L-WIXC architecture as a function of number of hops varying number of input wavelengths for (a) Coherent Case when N=4 (b) Incoherent Case when N=4 (c) Coherent Case when

N=8 (d) Incoherent Case when N=8 (e) Coherent Case when N=16 (f) Incoherent Case when N=16 (g) Coherent Case when N=24 (h) Incoherent Case when N=24 (i) Coherent Case when N=32 (j) Incoherent Case when N=32

From Fig 4.6 it is observed that, when the signal passes through more hops, additional power penalty occurs since the receiver sensitivity decreases due to induced crosstalk and noise through the system for maintaining the same BER level. It is also observed that between these two cases of coherent and incoherent crosstalk, the more power penalty is found in coherent case than incoherent case with same number of hops and the same number of wavelength channels. As the number of wavelength channel increases, the same amount of receiver power penalty is to be achieved by decreasing the number hops used in the system.

4.9 Power Penalty Trend for MWSF-based L-WIXC Architecture

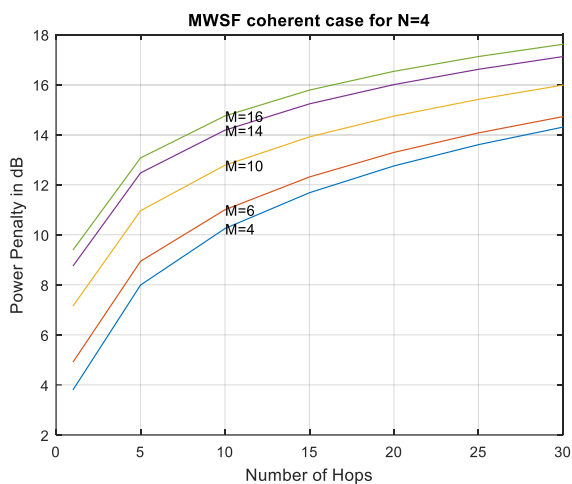
The BER versus Received Power graphs in Fig. 4.1(k) and 4.1(l) are analyzed varying number of wavelengths in a fiber using M=4, 6, 10, 14, 16 keeping number of fiber, N fixed to find out the received power variation at BER of 10^{-9} for various number of hops considering both coherent and incoherent cases of MWSF-based L-WIXC architectures. Then the same analysis is carried out for different values number of input fibers using N=4, 8, 16, 24 and 32 for all the above-mentioned number of wavelengths. The values of received power at BER of 10^{-9} are shown in Table VI.

TABLE VI
BER PERFORMANCE TREND FOR MWSF-BASED L-WIXC ARCHITECTURE

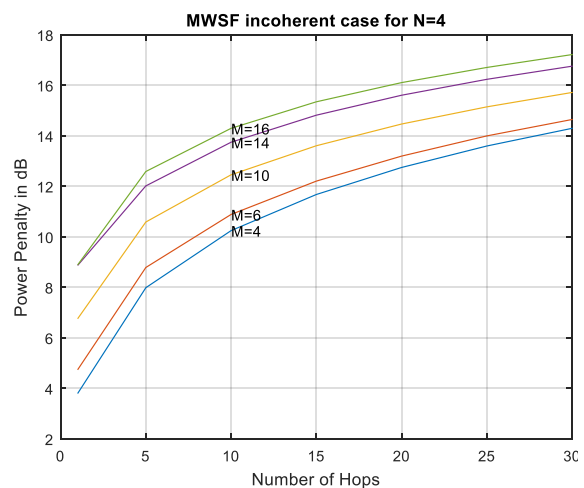
Number of Hops	N=4; M=4	N=4; M=10	N=4; M=16	N=16; M=4	N=16; M=10	N=16; M=16	N=32; M=4	N=32; M=10	N=32; M=16
MWSF-based Coherent Case									
1	-31.16	-27.81	-25.57	-28.85	-27.13	-25.32	-27.55	-26.47	-25.01
5	-26.97	-24.00	-21.89	-24.95	-23.37	-21.64	-23.77	-22.75	-21.36
10	-24.71	-22.18	-20.21	-23.03	-21.59	-19.96	-21.96	-21.01	-19.69

15	-23.28	-21.05	-19.18	-21.83	-20.5	-18.95	-20.85	-19.95	-18.69
20	-22.21	-20.22	-18.43	-20.94	-19.7	-18.21	-20.02	-19.18	-17.95
25	-21.36	-19.55	-17.84	-20.22	-19.06	-17.62	-19.37	-18.56	-17.37
30	-20.66	-18.98	-17.35	-19.62	-18.52	-17.14	-18.82	-18.04	-17.28
MWSF-based Incoherent Case									
1	-31.16	-28.20	-26.07	-28.85	-27.4	-25.75	-27.55	-26.67	-25.39
5	-26.97	-24.37	-22.37	-24.95	-23.62	-22.06	-23.77	-22.93	-21.72
10	-24.71	-22.5	-20.66	-23.03	-21.83	-20.37	-21.96	-21.19	-20.03
15	-23.28	-21.35	-19.61	-21.83	-20.73	-19.34	-20.85	-20.12	-19.01
20	-22.21	-20.49	-18.85	-20.94	-19.91	-18.58	-20.02	-19.34	-18.28
25	-21.36	-19.81	-18.25	-20.22	-19.26	-17.98	-19.37	-18.71	-17.69
30	-20.66	-19.24	-17.74	-19.62	-18.71	-17.48	-18.82	-18.19	-17.53

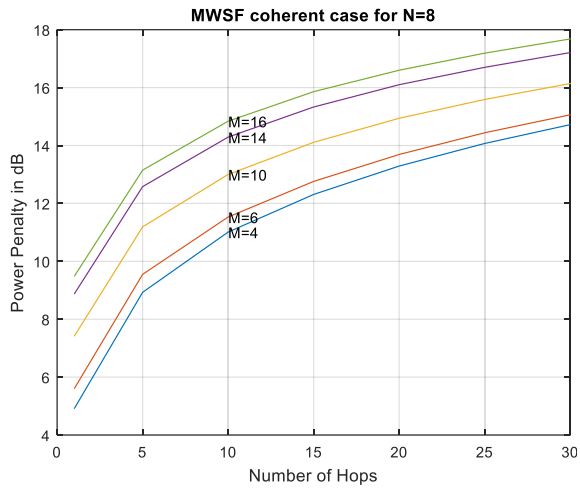
Power penalty performance trend for a WDM network using Share per Node L-WIXC architecture as a function of number of hops varying number of input wavelengths, M for (a) Coherent Case when N=4 (b) Incoherent Case when N=4 (c) Coherent Case when N=8 (d) Incoherent Case when N=8 (e) Coherent Case when N=16 (f) Incoherent Case when N=16 (g) Coherent Case when N=24 (h) Incoherent Case when N=24 (i) Coherent Case when N=32 (j) Incoherent Case when N=32 has been presented in Fig 4.7 below.



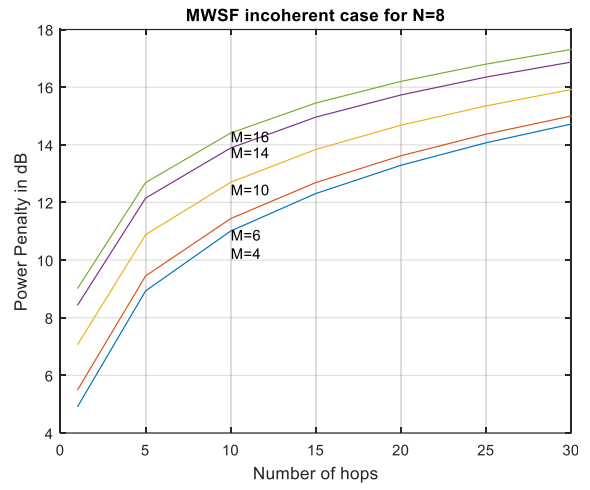
(a)



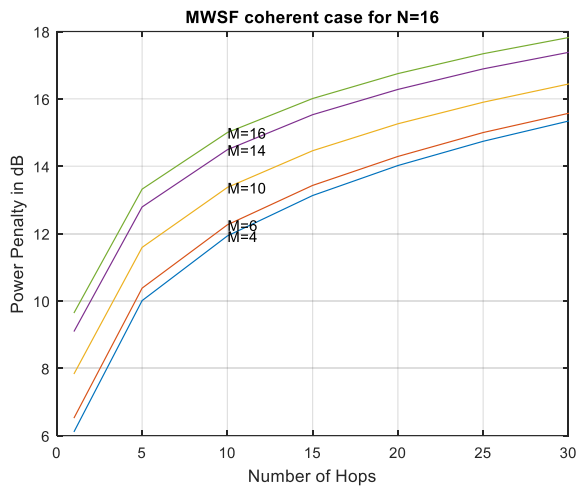
(b)



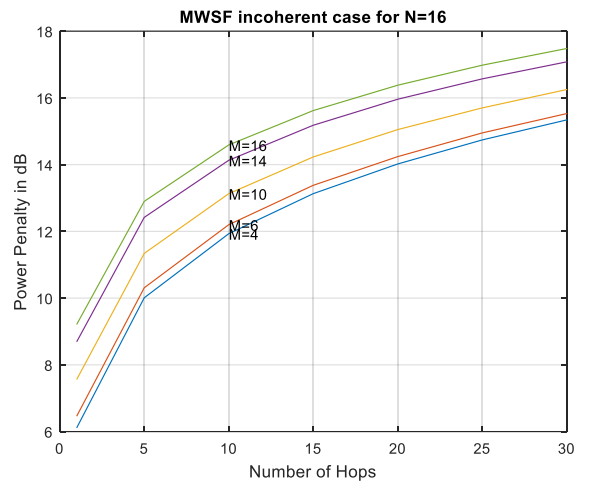
(c)



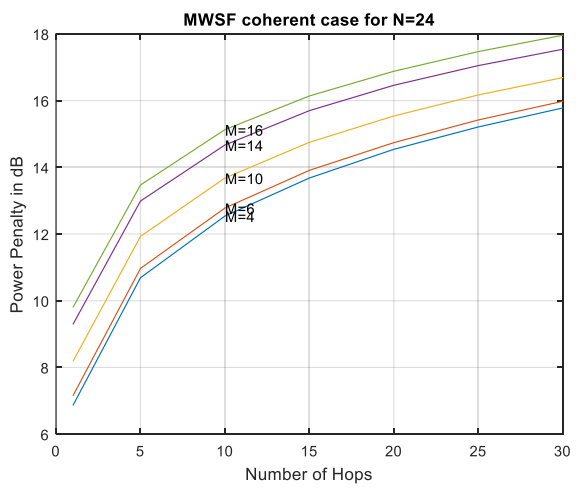
(d)



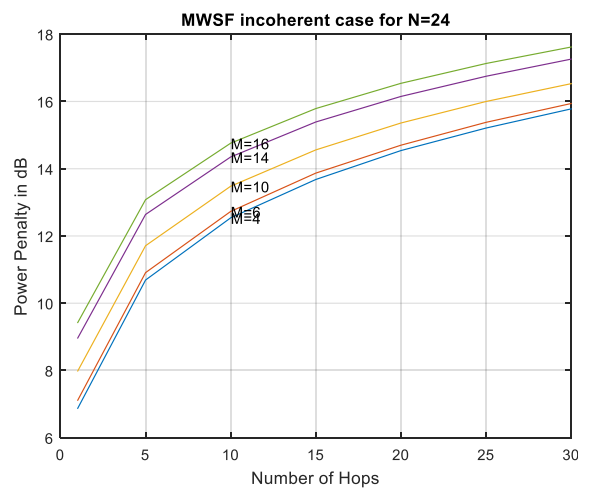
(e)



(f)



(g)



(h)

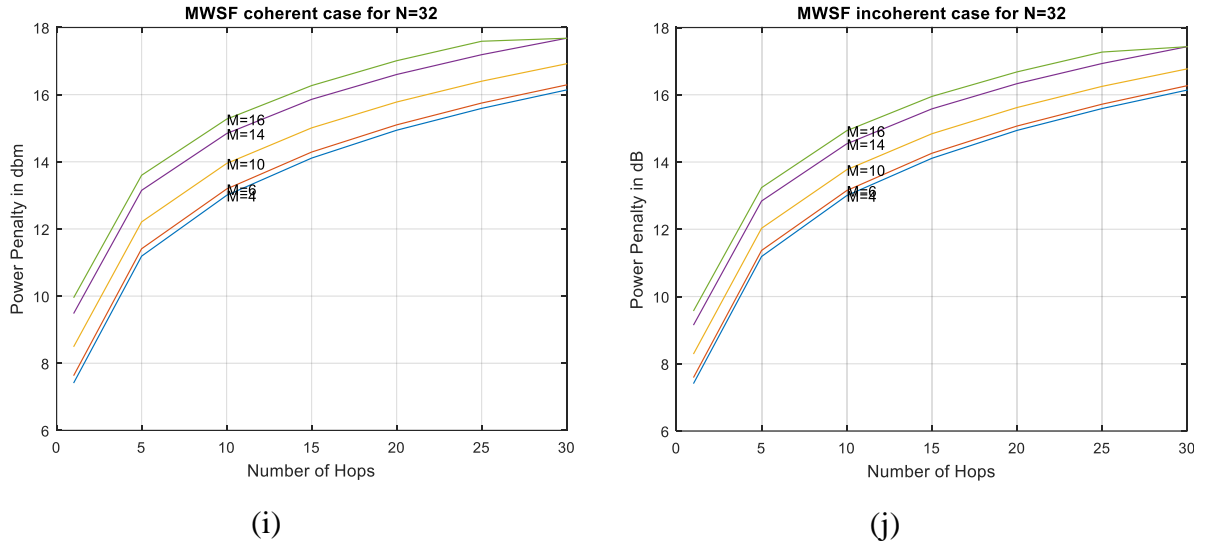


Fig. 4.7 Power penalty for a WDM network using **MWSF-based** L-WIXC architecture as a function of number of hops varying number of input wavelengths for (a) Coherent Case when N=4 (b) Incoherent Case when N=4 (c) Coherent Case when N=8 (d) Incoherent Case when N=8 (e) Coherent Case when N=16 (f) Incoherent Case when N=16 (g) Coherent Case when N=24 (h) Incoherent Case when N=24 (i) Coherent Case when N=32 (j) Incoherent Case when N=32

From Fig 4.7 it is observed that, when the signal passes through more hops, additional power penalty occurs since the receiver sensitivity decreases due to induced crosstalk and noise through the system for maintaining the same BER level. It is also observed that between these two cases of coherent and incoherent crosstalk, the more power penalty is found in coherent case than incoherent case with same number of hops and the same number of wavelength channels. As the number of wavelength channel increases, the same amount of receiver power penalty is to be achieved by decreasing the number hops used in the system.

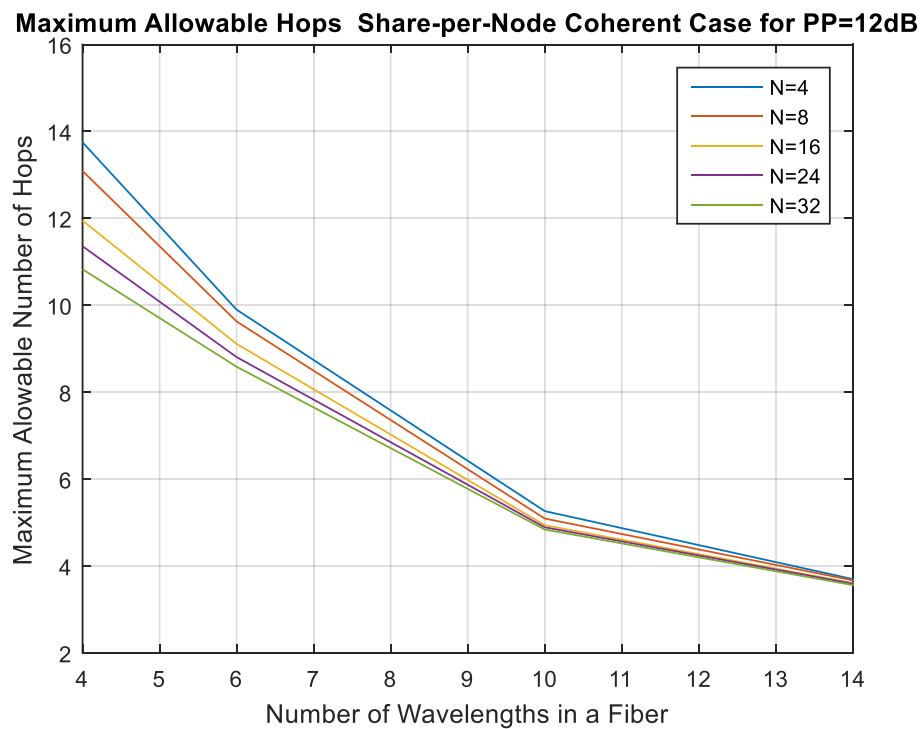
4.10 Maximum Allowable Number of Hops

A network designer needs to know how many hops the signal can travel at specific BER with the existing requirements of wavelength channels and input fibers while designing the WDM network. In this section, the maximum allowable number of hops for different

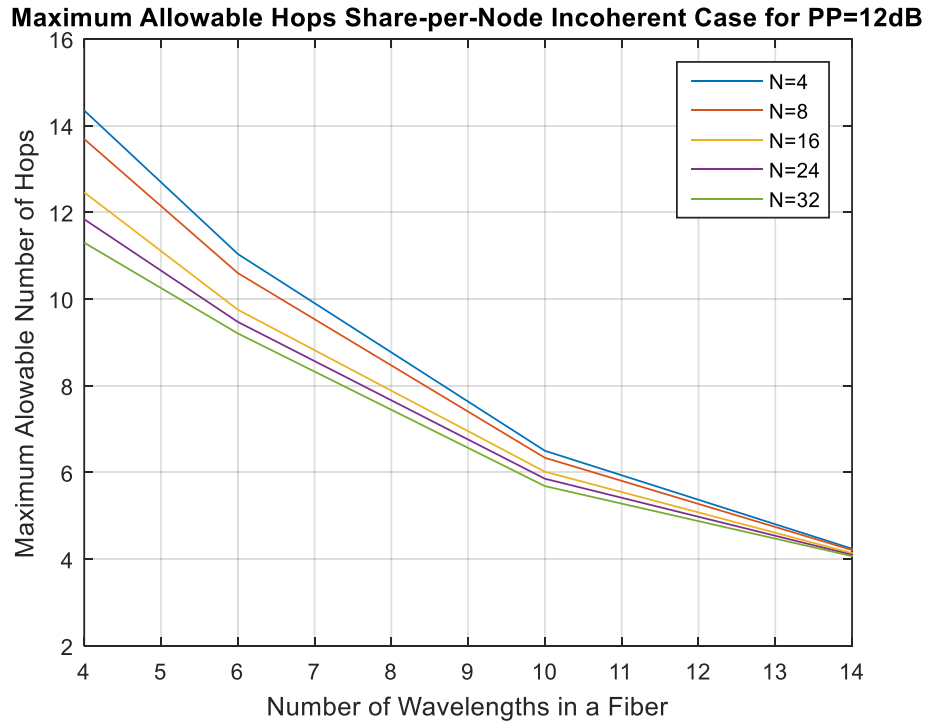
combinations of number of wavelengths in a fiber and number of input fibers are found when a WDM network is designed with L-WIXC architectures. Maximum allowable number of hops are found considering the sustainable power penalty level of 12 dB for both coherent cases and incoherent cases. The Comparative study of the system performance that is depicted for all architectures of L-WIXC can help the system designer to choose the effective one.

4.10.1 Designing a WDM Network with Share-per-Node Architecture

Maximum allowable number of hops that can be travelled by a WDM network designed with Share-per Node Architecture is graphically presented in fig. 4.8 using the power penalty performance curves presented in fig 4.2 (a)-(j). The numerical values of the hops that can be travelled by a signal at PP level of 12 dB are obtained and plotted as a function of number of wavelengths in a channel, M while varying number of input channels, N when $N=4, 8, 16, 24$ and 32 .



(a)

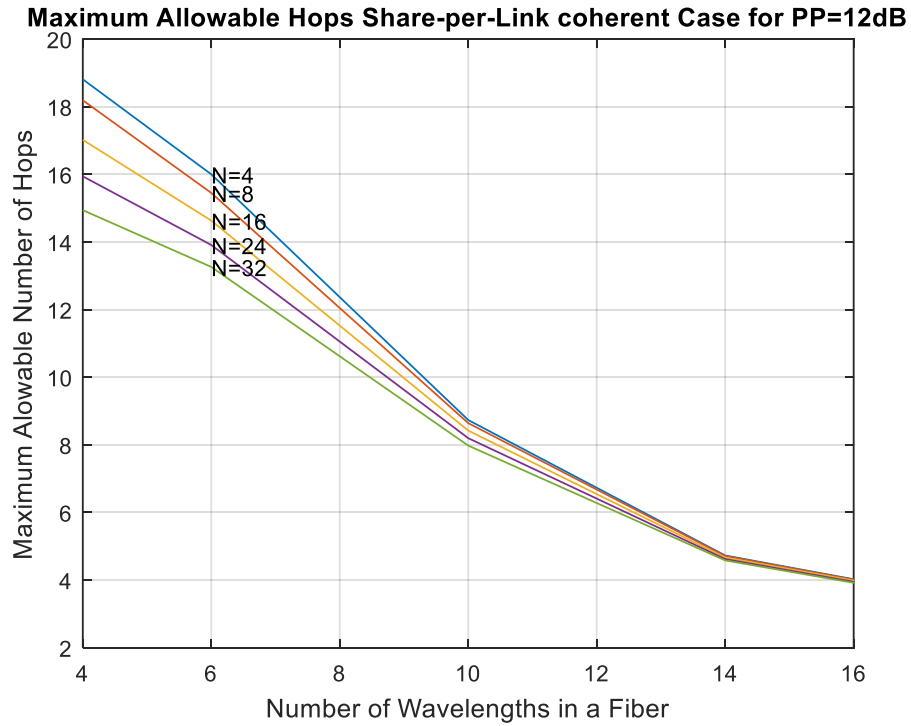


(b)

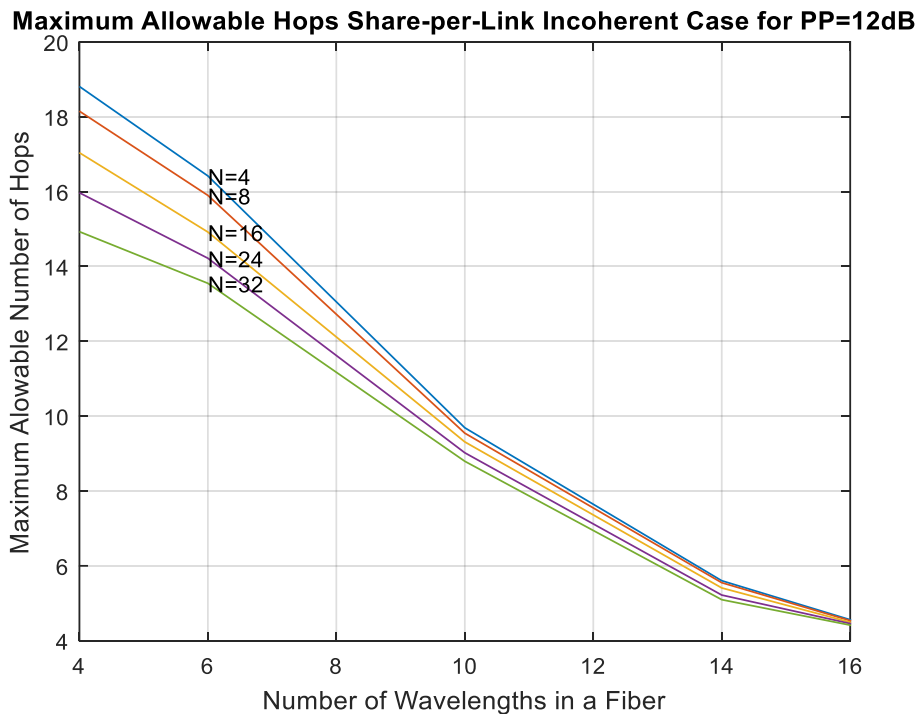
Fig. 4.8 Maximum allowable number of hops for a WDM network using Share-per-Node architecture (a) coherent case (b) incoherent case as a function of number of wavelengths in a channel varying number of input channels when PP=12 dB

4.10.2 Designing a WDM Network with Share-per-Link Architecture

Maximum allowable number of hops that can be travelled by a WDM network designed with Share-per Link Architecture is graphically presented in fig. 4.9 using the power penalty performance curves presented in fig 4.3 (a)-(j). The numerical values of the hops that can be travelled by a signal at PP level of 12 dB are obtained and plotted as a function of number of wavelengths in a channel, M while varying number of input channels, N when $N=4, 8, 16, 24$ and 32 .



(a)

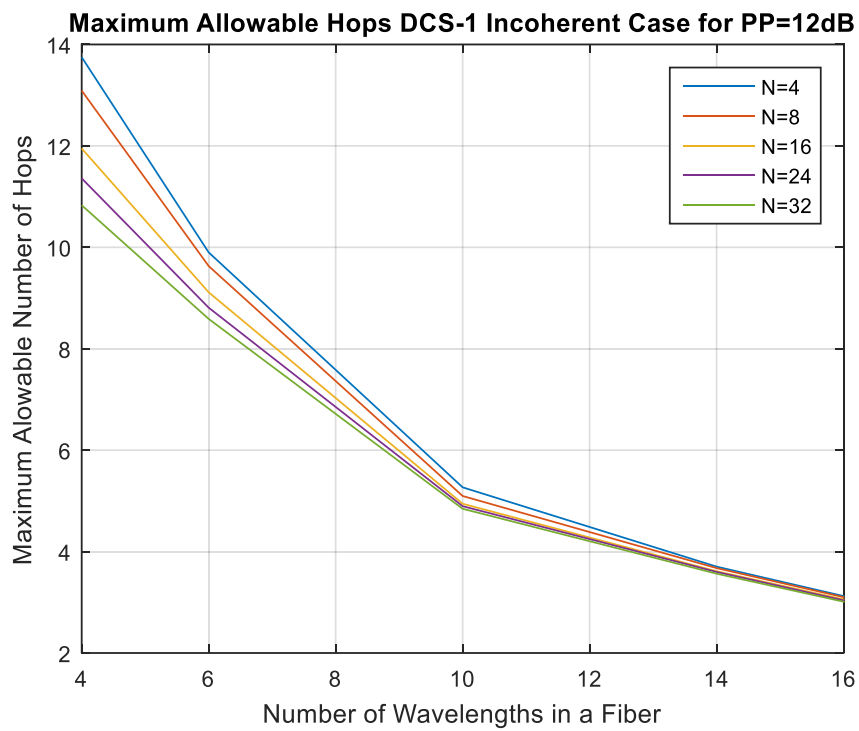


(b)

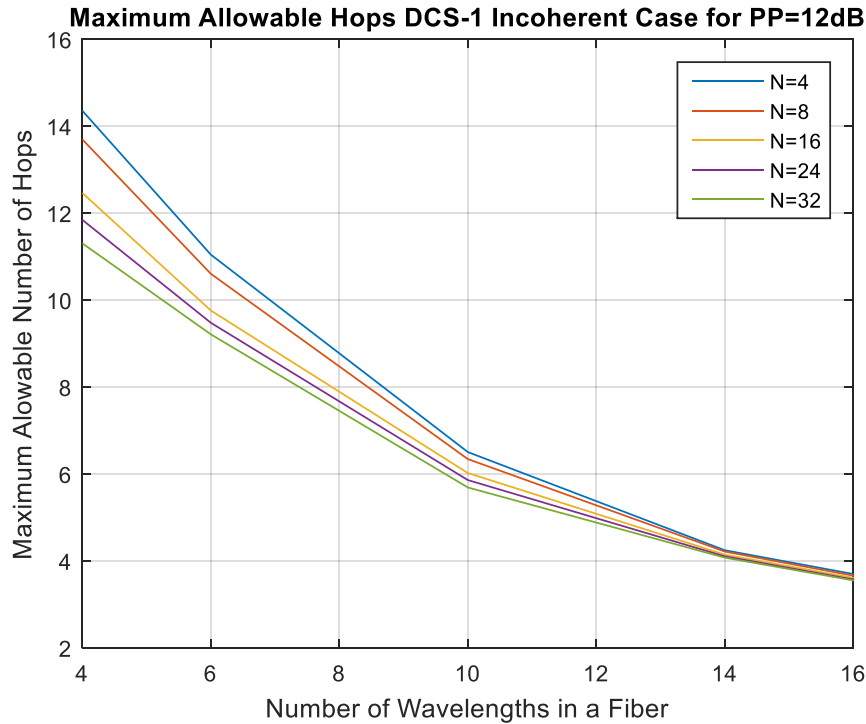
Fig. 4.9 Maximum allowable number of hops for a WDM network using Share-per-Link architecture (a) coherent case (b) incoherent case as a function of number of wavelengths in a channel varying number of input channels when PP=12 dB obtained from the plots of Fig. 4.3

4.10.3 Designing a WDM Network with DCS-1 Architecture

Maximum allowable number of hops that can be travelled by a WDM network designed with DCS-1 Architecture is graphically presented in fig. 4.10 using the power penalty performance curves presented in fig 4.4 (a)-(j). The numerical values of the hops that can be travelled by a signal at PP level of 12 dB are obtained and plotted as a function of number of wavelengths in a channel, M while varying number of input channels, N when $N=4, 8, 16, 24$ and 32 .



(a)

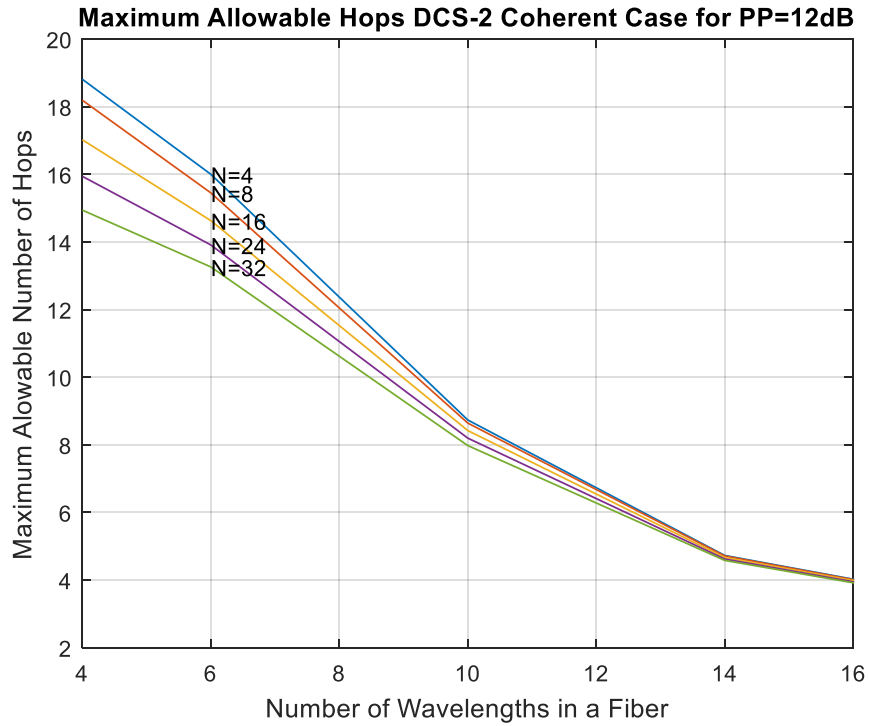


(b)

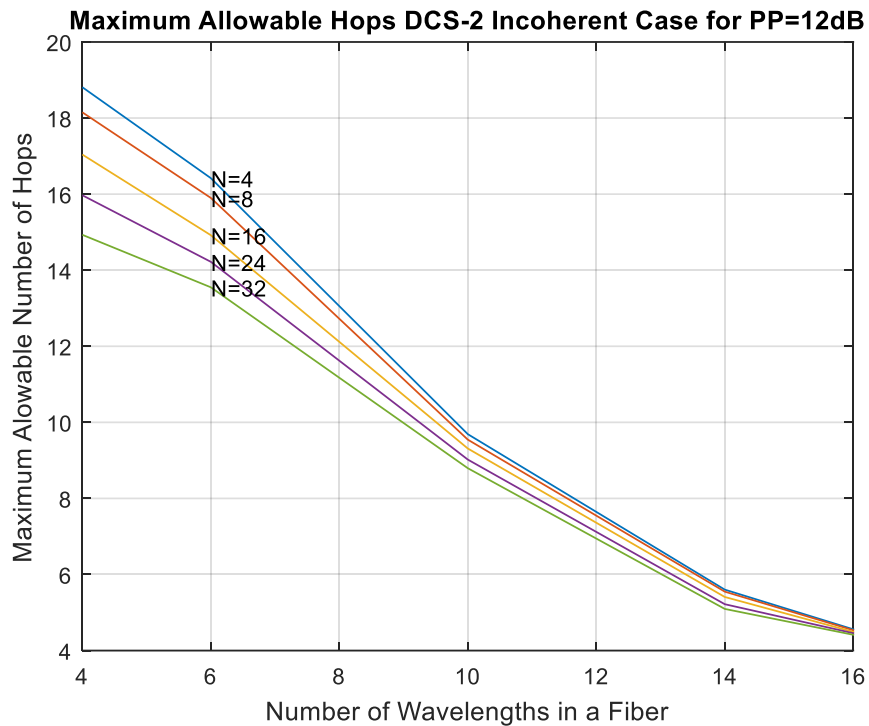
Fig. 4.10 Maximum allowable number of hops for a WDM network using DCS-1 architecture (a) coherent case (b) incoherent case as a function of number of wavelengths in a channel varying number of input channels when PP=12 dB obtained from the plots of Fig. 4.4

4.10.4 Designing a WDM Network with DCS-2 Architecture

Maximum allowable number of hops that can be travelled by a WDM network designed with DCS-2 Architecture has been graphically presented in fig. 4.11 using the power penalty performance curves presented in fig 4.5 (a)-(j). The numerical values of the hops that can be travelled by a signal at PP level of 12 dB are obtained and plotted as a function of number of wavelengths in a channel, M while varying number of input channels, N when N=4, 8, 16, 24 and 32.



(a)

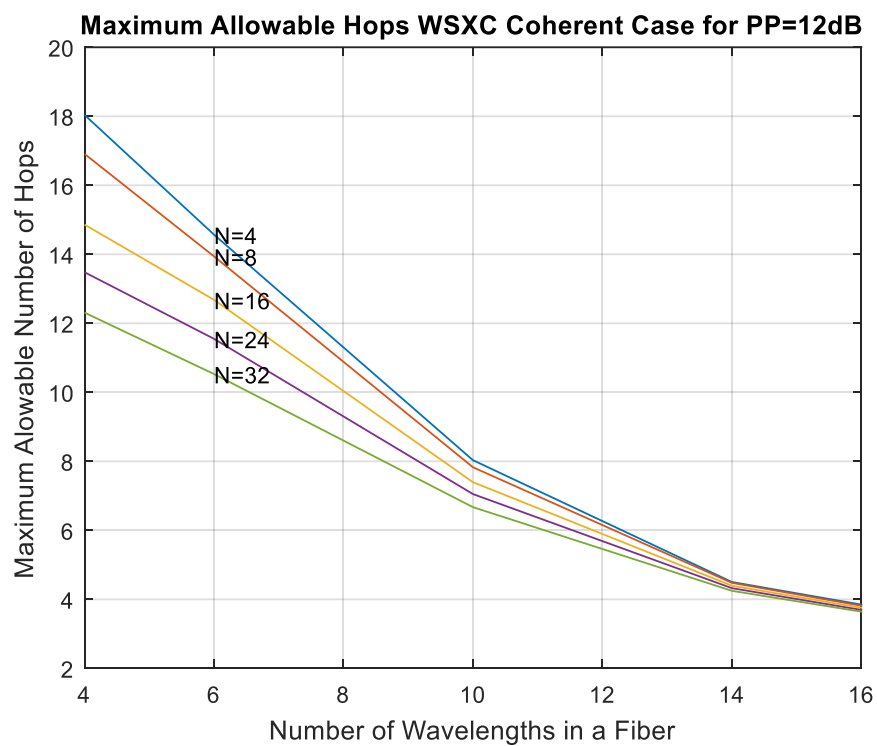


(b)

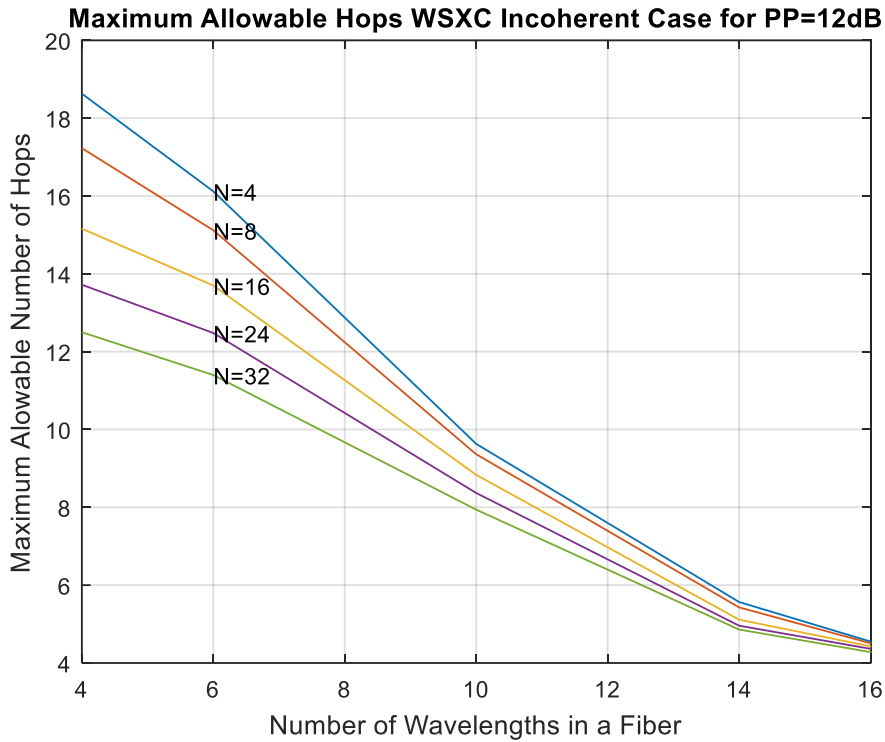
Fig. 4.11 Maximum allowable number of hops for a WDM network using DCS-2 architecture (a) coherent case (b) incoherent case as a function of number of wavelengths in a channel varying number of input channels when PP=12 dB obtained from the plots of Fig. 4.5

4.10.5 Designing a WDM Network with WS-based L-WIXC Architecture

Maximum allowable number of hops that can be travelled by a WDM network designed with WSXC Architecture is graphically presented in fig. 4.12 using the power penalty performance curves presented in fig 4.6 (a)-(j). The numerical values of the hops that can be travelled by a signal at PP level of 12 dB have been obtained and plotted as a function of number of wavelengths in a channel, M while varying number of input channels, N when $N=4, 8, 16, 24$ and 32 .



(a)

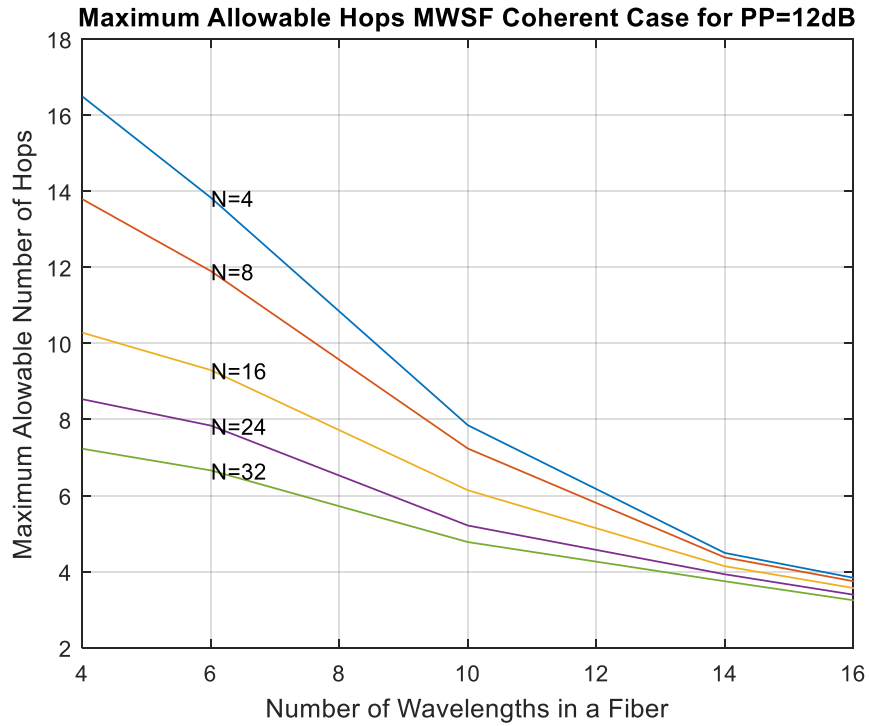


(b)

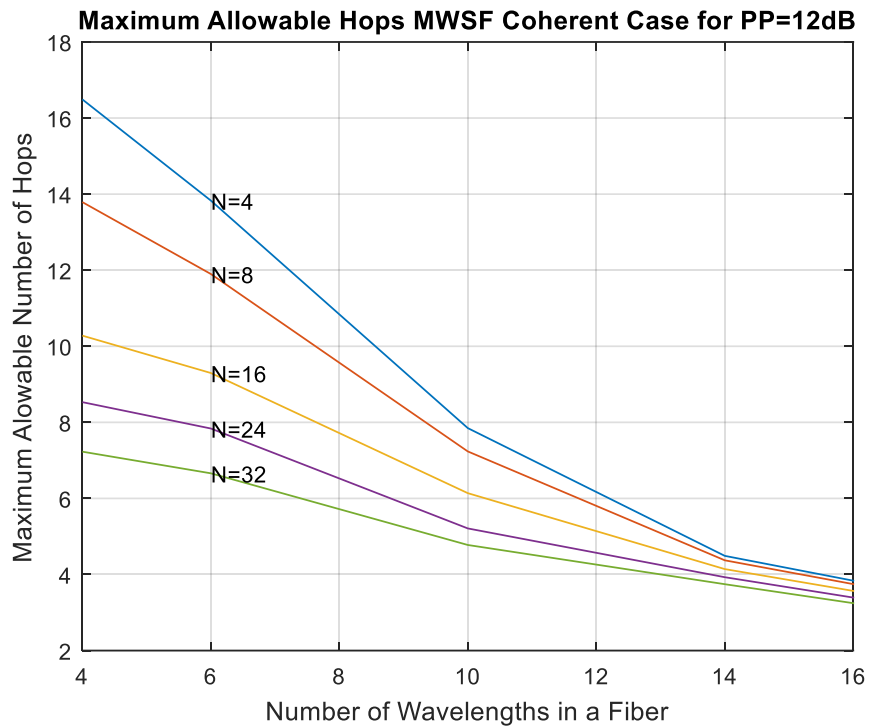
Fig. 4.12 Maximum allowable number of hops for a WDM network using WS-based L-WIXC architecture (a) coherent case (b) incoherent case as a function of number of wavelengths in a channel varying number of input channels when PP=12 dB obtained from the plots of Fig. 4.6

4.10.6 Designing a WDM Network with MWSF-based L-WIXC Architecture

Maximum allowable number of hops that can be travelled by a WDM network designed with MWSF-based L-WIXC Architecture is graphically presented in fig. 4.13 using the power penalty performance curves presented in fig 4.7 (a)-(j). The numerical values of the hops that can be travelled by a signal at PP level of 12 dB are obtained and plotted as a function of number of wavelengths in a channel, M while varying number of input channels, N when N=4, 8, 16, 24 and 32.



(a)



(b)

Fig. 4.13 Maximum allowable number of hops for a WDM network using MWSF OXC architecture (a) coherent case (b) incoherent case as a function of number of wavelengths in a channel varying number of input channels when PP=12 dB obtained from the plots of Fig. 4.7

Fig 4.8 to Fig 4.13 are obtained for determining the maximum allowable number of hops that a signal can travel sustaining specific power penalty level at BER of 10^{-9} considering various number of wavelengths in a fiber and various number of input fiber using Fig. 4.2-4.7. The Comparative study of the system performance that is depicted for all architectures of L-WIXC can help the system designer to choose the desirable and effective combination while designing an all-optical WDM network.

4.11 Comparison of Maximum Allowable Hops

The comparative study of the system performance is presented for all the various architectures of L-WIXC. This comparison will help the system designer to choose the desirable and effective combination while designing an all-optical WDM network.

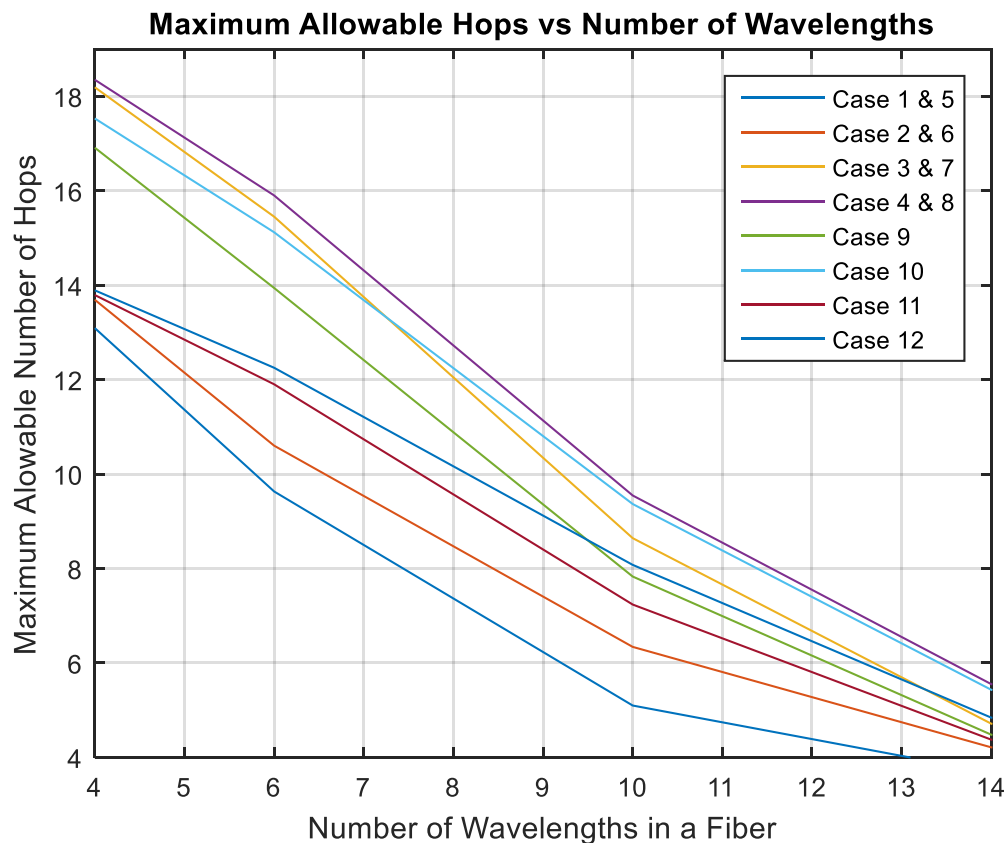


Fig. 4.14 Comparison of variation of maximum allowable number of hops with number of input wavelengths per fiber for all architectures of L-WIXC at BER= 10^{-9} (when Number

of Input Fibers $N=8$) considering cases 1. Share per node coherent case 2. Share per node incoherent case, 3. Share per link coherent case, 4. Share per link incoherent case, 5. DCS-1 coherent case, 6. DCS-1 incoherent case, 7. DCS-2 coherent case, 8. DCS-2 incoherent case, 9. Wavelength switch OXC coherent case, 10. Wavelength switch OXC incoherent case, 11. MWSF coherent case, 12. MWSF incoherent case.

Figure 4.14 shows the comparison of performance of a multi-hop WDM network taking all the L-WIXC architectures into consideration depending on the analysis presented in section 4.10. In all cases number of converters per link are assumed to be 4 and number of input fibers are 8. From this figure we observe that in all cases maximum allowable number of hops decreases with the increase of number of wavelengths per fiber. Share per link Incoherent Case and DCS-2 Incoherent case shows the best performance in respect of travelling further hops compared to all the cases while using same number of wavelengths per fiber.

4.12 Summery

The combined effect of noise generated by optical amplifiers as well as crosstalk contributions by L-WIXC architectures on the BER performance in a multi-hop WDM network is studied. Analyzing the BER performance trend varying the system parameters as number of hops, number of wavelengths and number of input fibers, power penalty (PP) performance trend is evaluated. From the PP trends, maximum allowable number of hops for specific number of wavelength channels and number of input fibers in multi-hop WDM network is presented and analyzed. Lastly, a comparative study is presented for the performance analysis of all the architectures in terms of maximum allowable number of hops in the network.